N66 34431

MSFC COMPUTER PROGRAMS UTILIZED IN THE THERMAL DESIGN AND ANALYSIS OF SATELLITES

William C. Snoddy
MSFC

MSFC Computer Programs Utilized in the Thermal Design and Analysis of Satellites

William C. Snoddy
MSFC

INTRODUCTION

Three IBM 7094 computer programs used in the thermal design of spacecraft will be discussed. The first program is one used for integrating spectral reflectance or emittance data to obtain total reflectance or emittance. The second program calculates the percent time a satellite spends in the earth's shadow during a revolution about the earth. And the third program is called our General Space Thermal Program and is used to calculate satellite temperatures throughout a revolution about the earth.

SPECTRAL INTEGRATION PROGRAM

This program integrates spectral radiometric data with respect to blackbody radiation at any temperature or with respect to the Johnson solar radiation curve. One of the advantages of this program over similar programs is the simplicity of data input. Only those data points are needed which together with linear interpolation between points will define the spectral data curve. For example, the curves shown in figure 1 were entered into the computer by reading only those points marked on the curves. These points were chosen because it can be seen that if they are connected by straight lines (which the computer does when it interpolates linearly) the result will closely follow the original curves. Thus, for much spectral data it is necessary to enter only four or five points into the computer.

Figure 2 is the computer printout for the data taken from the upper curve in figure 1. First is given the identification of the sample and then the input data is printed out. Given any two of the following, (1) emittance, (2) reflectance, and (3) transmittance, the computer will calculate the third using Kirchoff's Law. In this case the sample was opaque so that the transmittance was assumed to be zero and thus the emittance was calculated. The integration of this data with respect to solar-type radiation was of interest and therefore this integration was performed with respect to a blackbody curve at 5800°K and 6000°K (for other temperatures it is only necessary to input the temperatures themselves) and also with respect to the Johnson solar curve which is stored in the computer.. The column on the right gives the percent of the energy outside the region covered by the data (in this case less than 0.32 microns and greater than 3.0 microns). The center three columns give the integrated emittance (which is equal to the absorptance by Kirchoff's Law) for each of the three cases of interest and for various means of extrapolation to cover the wavelengths outside the data region. In the first of these columns the integrated value is shown where a "straight" extrapolation is used. That is the radiometric values for the two end data points are used as the extrapolated values. In the next column results are given for an extrapolation made by fitting a curve to the data. And in the next column the results are shown for the case where no extrapolation is made or it can be thought of as an extrapolation made such that it does not alter the value of the integration. It might be noted that in this case, depending on the solar model (blackbody or Johnson) and manner of extrapolation, a solar absorptance ranging from 0.32 to 0.39 was obtained.

The 7094 computer together with a S.C. 4020 also plots the data as shown in figure 3 (reflectance) and figure 4 (emittance or absorptance).

The lower curve in figure 1 was integrated to obtain total emittance with respect to various blackbody temperatures and by mistake the Johnson solar curve. These results are given in figure 5 where the results for the Johnson curve indicates problems caused by extrapolation over large regions. Plots of the spectral reflectance and emittance are given in figures 6 and 7 respectively. By using the results of this program and fitting a curve to the total emittance as a function of temperature the variation of emittance with respect to temperature could easily be included in thermal computer programs.

SHADOW-SUNLIGHT PROGRAM

In this program information regarding the passage of a satellite through the earth's shadow (figure 8) is obtained for use in satellite thermal design and analysis work. The effect that variations in the percent of the time that a satellite spends in the earth's shadow per revolution can have on temperature of a satellite is shown in figure 9 where a close correlation between this parameter and the internal temperature of Explorer VII during 320 days of orbiting can be seen.

Great pains have been taken with this program to simplify data input as much as possible. For prelaunch studies it is usually convenient to input the data shown in figure 10 and for postlaunch calculations the alternate form of data input given in figure 11 may be used, since these parameters are usually readily available for any orbiting satellite. From this input the program calculates, among other things, the orbital positions where the satellite enters and leaves the earth's shadow, and the percent time spent in the shadow. Calculations are also made for successive days by extrapolation of the orbital elements considering perturbations caused by the oblateness of the earth. To avoid having to load the position of the sun into the computer from the ephemeris, equations were derived and included in the program which calculate the right ascension and declination of the sun considering such parameters as leap years.

Some of the results of the program are shown in figure 12. The top curve is the percent of time spent in the sunlight per revolution as a function of days after launch for the Explorer VII satellite. This curve was obtained in one computer run consisting of 365 complete calculations and required about one minute of machine time giving a running time of about 1/6 second per calculation. The orbital parameters were extrapolated for the entire year and it was later determined that these extrapolated results were in good agreement with results obtained using actual orbital parameters. In the lower part of figure 12 is plotted additional computer output, namely, the orbital position of ingress into the earth's shadow, egress from the shadow, and perigee relative to the ascending node and as a function of days after launch. The position is given in terms of time (in minutes) required for the satellite to travel from the ascending node to the point of interest and an error analysis indicates accuracy to less than 10 seconds. This accuracy was further verified by visual observations of Echo I.

This type of graph is especially useful in determining what part of the orbit a given tracking station will be able to "see" and thus aid in planning tracking and performing data analysis. This is accomplished by the fact that a tracking station at some fixed geographical latitude can at best "see" only a certain part of the satellite's orbit on any given day. In the case of Explorer VII and the Huntsville station, that part of the orbit approximately between the two lines on the graph in figure 12 could be tracked at some time during the day. Thus initially Huntsville could track only during the daylight portions of the orbit. On about 20 days after launch we could catch the satellite as it went into the earth's shadow and around 50 days after launch we could track it as it was leaving the shadow. Knowing this information ahead of time, tracking at the Huntsville station was coordinated throughout the year such that special effort could be made to obtain data at times of particular interest such as ingress, egress, and maximum and minimum sunlight conditions.

GENERAL SPACE THERMAL PROGRAM

MSFC has been involved in the thermal design of several spacecraft including Explorers I, III, IV, VII, VIII, and XI; Pioneers III and IV; Saturn SA-V Payload; and the Meteoroid Measurement Satellite to be flown on Saturn around the end of this year. Some of these spacecraft are shown in figure 13. It was found that weeks and even months were often required to set up and debug each of the computer programs used for the thermal design and evaluation of each of the spacecraft. Thus was born the idea of a computer program which could be utilized to minimize the time and effort involved in obtaining theoretical results and at the same time maximize the degree of sophistication which can be efficiently used for such calculations.

The basic general equation used in the General Space Thermal Program is given in figure 14. The equation is a first order fourth degree differential equation representing the instantaneous heat flow into and out of a section of the spacecraft the temperature of which is assumed to be such that it can be represented by one "effective temperature." The computer will automatically set up "n" such equations depending on how many sections the spacecraft must be divided in order that the resulting set of equations will serve sufficiently as an analytical model. The first term on the right in the equation represents the solar flux absorbed by the section, the next term is the earth albedo flux absorbed, next the earth infrared radiation term, then radiation away from the surface to space, internal heat generation, and finally conduction and radiation exchange with all the other sections. The bracketed factors are treated as separate functions which are dependent on the specific makeup of each section.

The manner in which the program is organized is shown in figure 15. The program includes many special subroutines which can be used in calculating the separate functions (A's and Q's). Each of the subroutines are discussed briefly below.

"D" = determines whether the satellite is in the earth's shadow at each calculation point in the orbit

"PS" = determines the angle between perigee and the sun in the plane of the orbit

"$F_{\gamma,h}$" = calculates the geometry factor between a flat plate or the sides of a cylinder and the earth as a function of altitude and orientation.

"g" = calculates the geometry factor between a sphere and the earth as a function of altitude

"h" = calculates the altitude of the satellite as a function of position in orbit

MAS = determines the angle between M, a vector defining the orientation of a section of the spacecraft, and S, a vector toward the sun

RAM = calculates the angle between the radius vector to the satellite and the vector M as a function of position in orbit

RAS = calculates the angle between the radius vector and a vector toward the sun

The F subroutine might be of particular interest and its derivation is as follows: The geometry for planetary thermal radiation to a cylinder is shown in figure 16. The geometry factors for various orientation and altitudes were calculated using a lengthly numerical progress by Ballinger, et.al. (references 1 and 2) and part of their results is shown in figure 17. In order to most efficiently enter these results into the program with an overall accuracy of better than two percent, a two variable curve fit was made such all the information in figure 17 is contained in one fifth degree polynomial the coefficients of which are each fourth degree polynomials (figure 18). Such an efficient means of calculating the geometry factor allows the luxury of being able to combine the flux calculations directly into the general program itself and thus reduce data handling and overall time required to obtain results.

It was further found that the albedo flux could be calculated for the sides of a cylinder (or a flat plate) simply by multiplying the infrared geometry factor ($F_{\gamma h}$) by the cosine of RAS and ignoring variations in the "azimuth" angle ψ (figure 19) and the fact that the flux is actually a very complicated function of RAS. This process gives maximum errors of around 5% as shown in figure 20 where the dashed curves represent the results obtained by this method and the solid curves represent the "true" results from references 1 and 2. It might be noted that during a complete revolution about the earth the errors tend to cancel out.

The method used to integrate the set of "n" first order differential equation is the Kutta-Simpson one-third rule illustrated in figure 21. In order to reduce running time a method of varying the integration time step throughout a run was incorporated. This prevents the program from "blowing up" and decreasing computation times by factors of 10 or more in some cases.

As an example of the simplicity of using this program the case of a space-fixed hollow cube in orbit was considered (figure 22). The only information needed to set up the program is given in figure 23 and input data for a run is shown in figures 24 and 25. The conduction and radiation coefficients between sections are entered by use of a matrix (figure 25) and each value is given twice (i.e. $R_{ij} = R_{ji}$) allowing the computer to perform a check on data input. The results for this case are shown in figure 26.

Thus by use of this program it is possible to set up and obtain fairly sophisticated theoretical results from a computer program within 24 hours in many cases.

REFERENCES

1. Ballinger, J. C., Elizalda, J. C., Garcia-Varela, R. M., and Christensen, E. H.: "Environmental Control Study of Space Vehicles," Part II (Thermal Environment of Space), Convair (Astronautics) Division, General Dynamics Corporation, November 1960.

2. Ballinger, J. C. and Christensen, E. H.: "Environmental Control Study of Space Vehicles," Part II, Supplement A, Convair (Astronautics) Division, General Dynamics Corporation, January 1961.

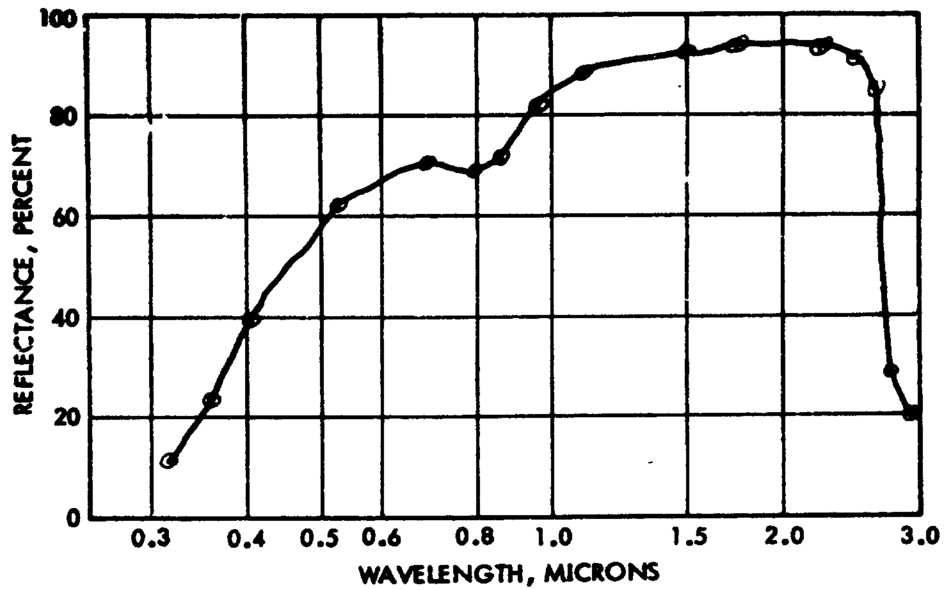

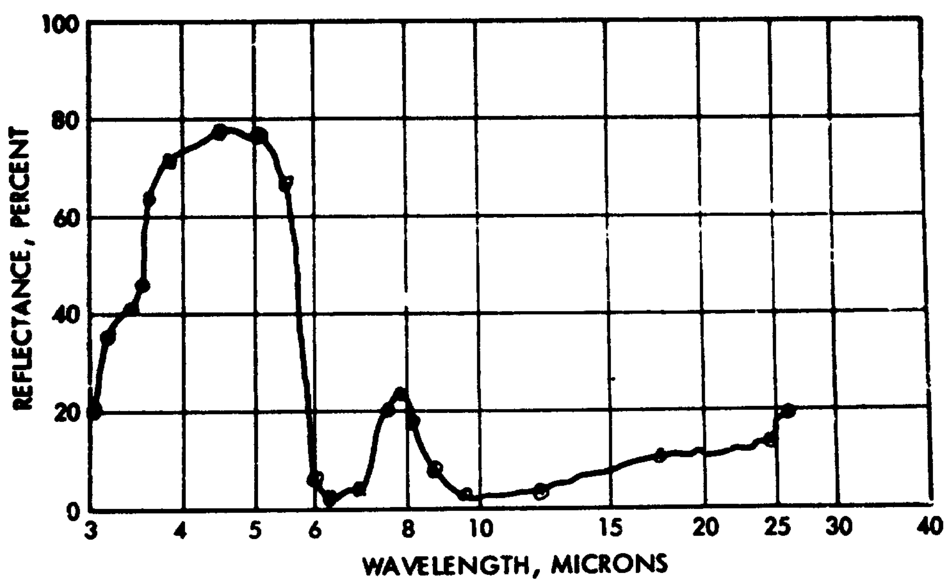

5557 Aluminum Alloy, Oxalic Acid Electrolyte
(Table III-7, Sample No. 13)

Figure 1

5557 ALUMINUM ALLOY, OXALIC ACID ELECTROLYTE (SOLAR)

WAVE LENGTH	EMITTANCE	REFLECTANCE	TRANSMITTANCE
0.320	0.900	0.100	0.
0.360	0.780	0.220	0.
0.400	0.600	0.400	0.
0.530	0.380	0.620	0.
0.700	0.300	0.700	0.
0.800	0.320	0.680	0.
0.880	0.290	0.710	0.
0.980	0.180	0.820	0.
1.100	0.110	0.890	0.
1.500	0.080	0.920	0.
1.800	0.070	0.930	0.
2.300	0.080	0.920	0.
2.670	0.100	0.900	0.
2.800	0.150	0.850	0.
2.900	0.710	0.290	0.
3.000	0.800	0.200	0.

T	STRAIGHT EXTRAPOLATION	CURVED EXTRAPOLATION	NO EXTRAPOLATION	PCT. BLACK BODY NOT COVERED
5000.	0.36	0.38	0.32	7
6000.	0.37	0.39	0.33	7
JOHNSON SOLAR CURVE	0.34	0.36	0.32	4

FILM PRINTED

Figure 2

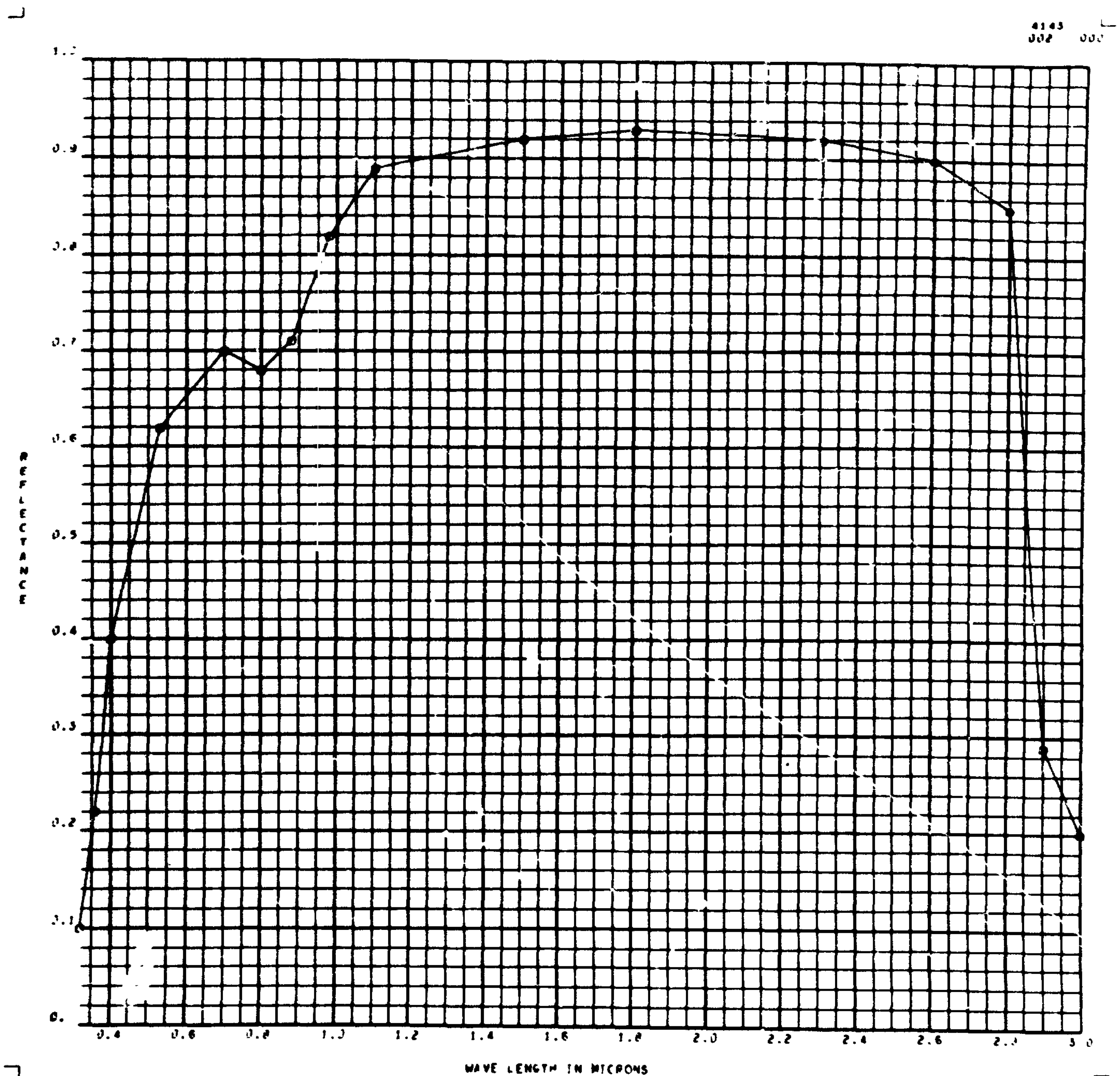
4143
002 000
REFLECTANCE
1.0
0.9
0.8
0.7
0.6
0.5
0.4
0.3
0.2
0.1
0.
0.4
0.6
0.8
1.0
1.2
1.4
1.6
1.8
2.0
2.2
2.4
2.6
2.8
3.0
WAVE LENGTH IN MICRONS

Figure 3

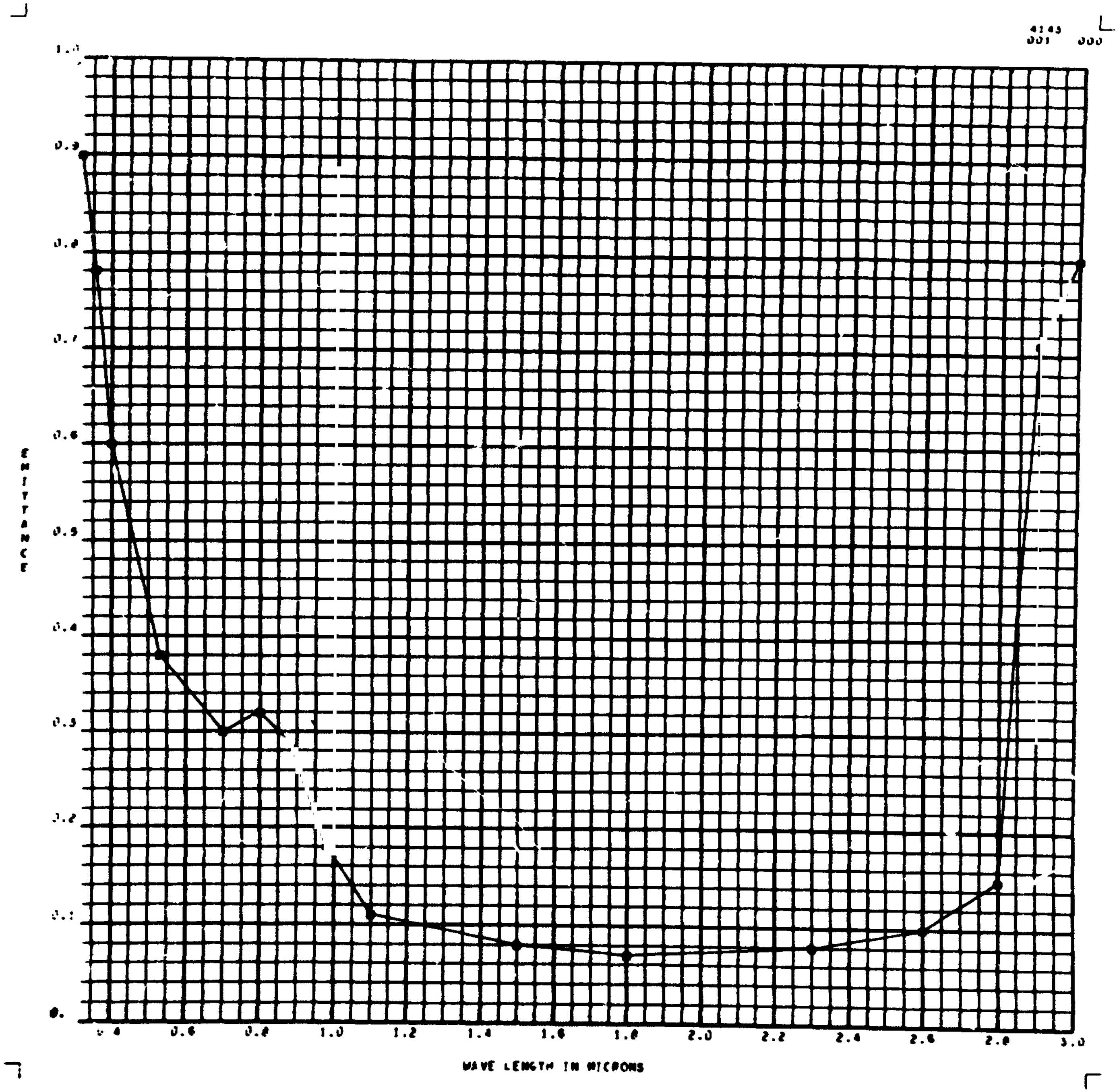
EMITTANCE
WAVE LENGTH IN MICRONS
1.0
0.9
0.8
0.7
0.6
0.5
0.4
0.3
0.2
0.1
0.
0.4
0.6
0.8
1.0
1.2
1.4
1.6
1.8
2.0
2.2
2.4
2.6
2.8
3.0

Figure 4

5557 ALUMINUM ALLOY, OXALIC ACID ELECTROLYTE (1R)

WAVE LENGTH	EMITTANCE	REFLECTANCE	TRANSMITTANCE
3.000	0.800	0.200	0.
3.200	0.630	0.370	0.
3.500	0.590	0.410	0.
3.600	0.550	0.450	0.
3.700	0.360	0.640	0.
3.900	0.280	0.720	0.
4.500	0.210	0.790	0.
5.100	0.220	0.780	0.
5.500	0.330	0.670	0.
6.000	0.950	0.050	0.
6.500	0.980	0.020	0.
7.500	0.960	0.040	0.
7.600	0.800	0.200	0.
7.900	0.780	0.220	0.
8.100	0.810	0.190	0.
8.700	0.920	0.080	0.
9.600	0.980	0.020	0.
12.500	0.970	0.030	0.
17.500	0.900	0.100	0.
24.500	0.860	0.140	0.
26.000	0.810	0.190	0.

T	STRAIGHT EXTRAPOLATION	CURVED EXTRAPOLATION	NO EXTRAPOLATION	PCT. BLACK BODY NOT COVERED
200.	0.88	0.66	0.91	34
300.	0.89	0.81	0.90	15
400.	0.84	0.80	0.84	8
500.	0.78	0.76	0.77	5
JOHNSON SOLAR CURVE	0.79	0.99	0.41	98

FILM PRINTED

Figure 5

4143
002 000

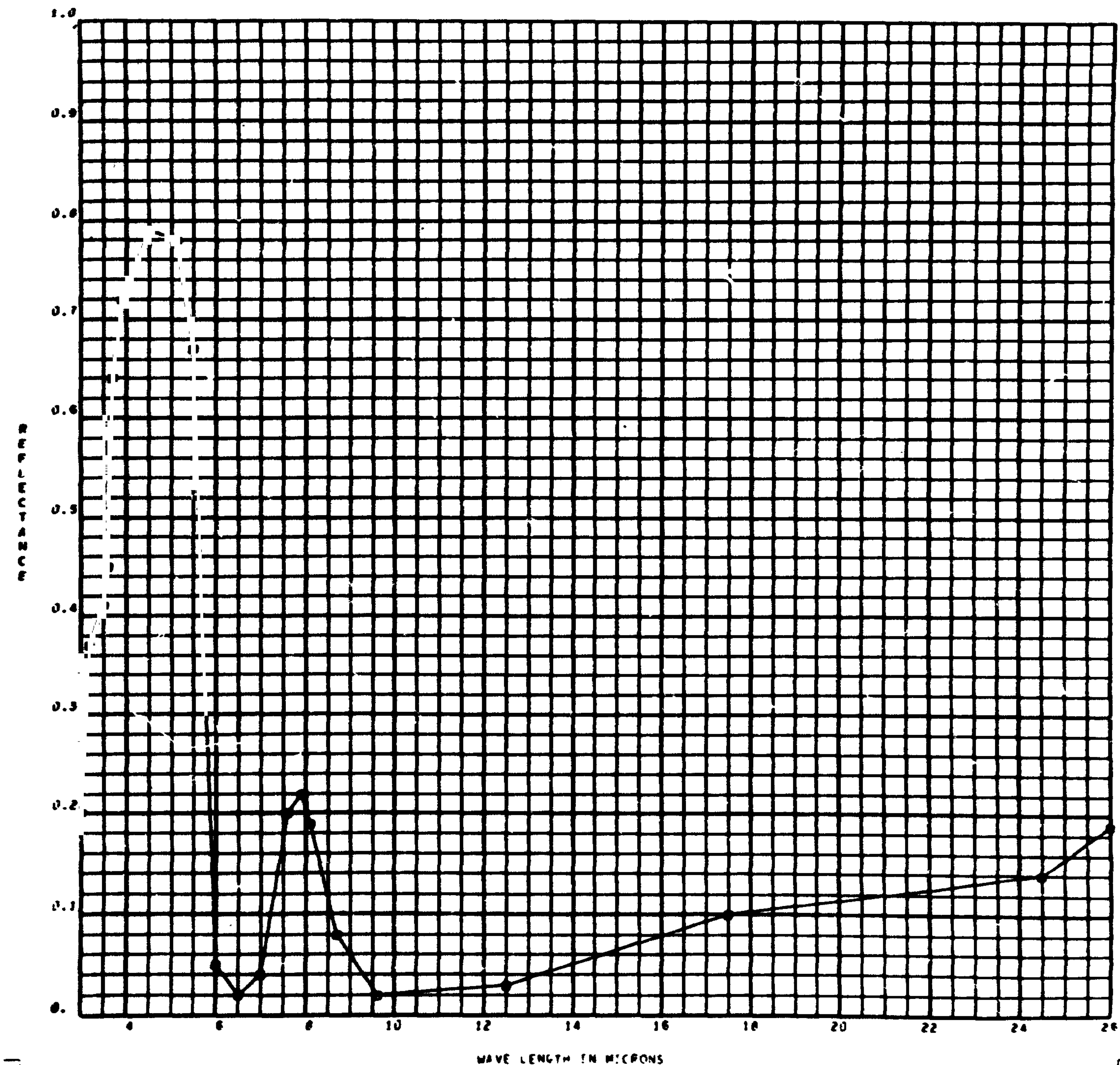

REFLECTANCE
1.0
0.9
0.8
0.7
0.6
0.5
0.4
0.3
0.2
0.1
0.
4
6
8
10
12
14
16
18
20
22
24
26
WAVE LENGTH IN MICRONS

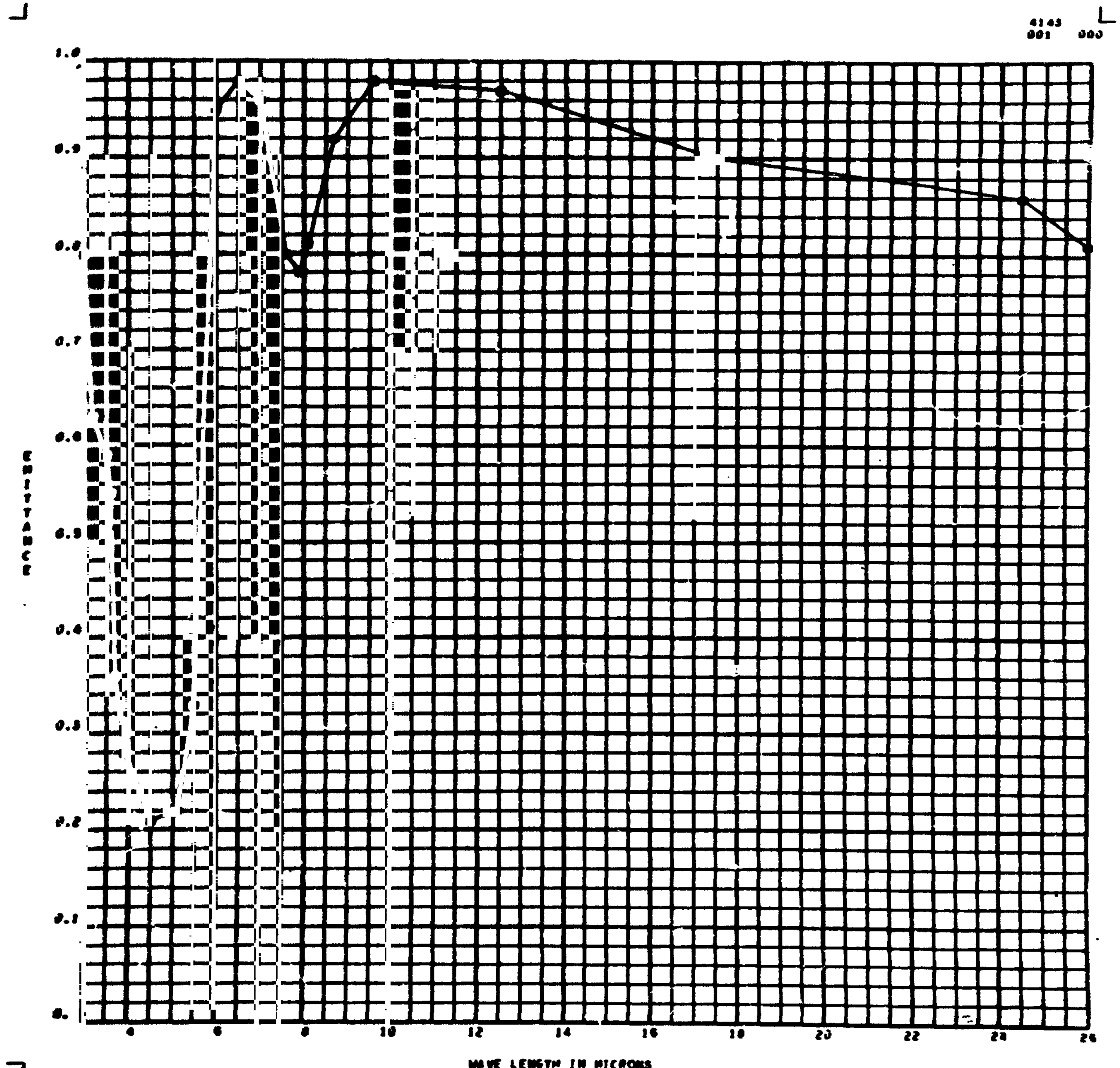
4143
001 000
1.0
0.9
0.8
0.7
0.6
0.5
0.4
0.3
0.2
0.1
0.
EMITTANCE
4
6
8
10
12
14
16
18
20
22
24
26
WAVE LENGTH IN MICRONS

Figure 7

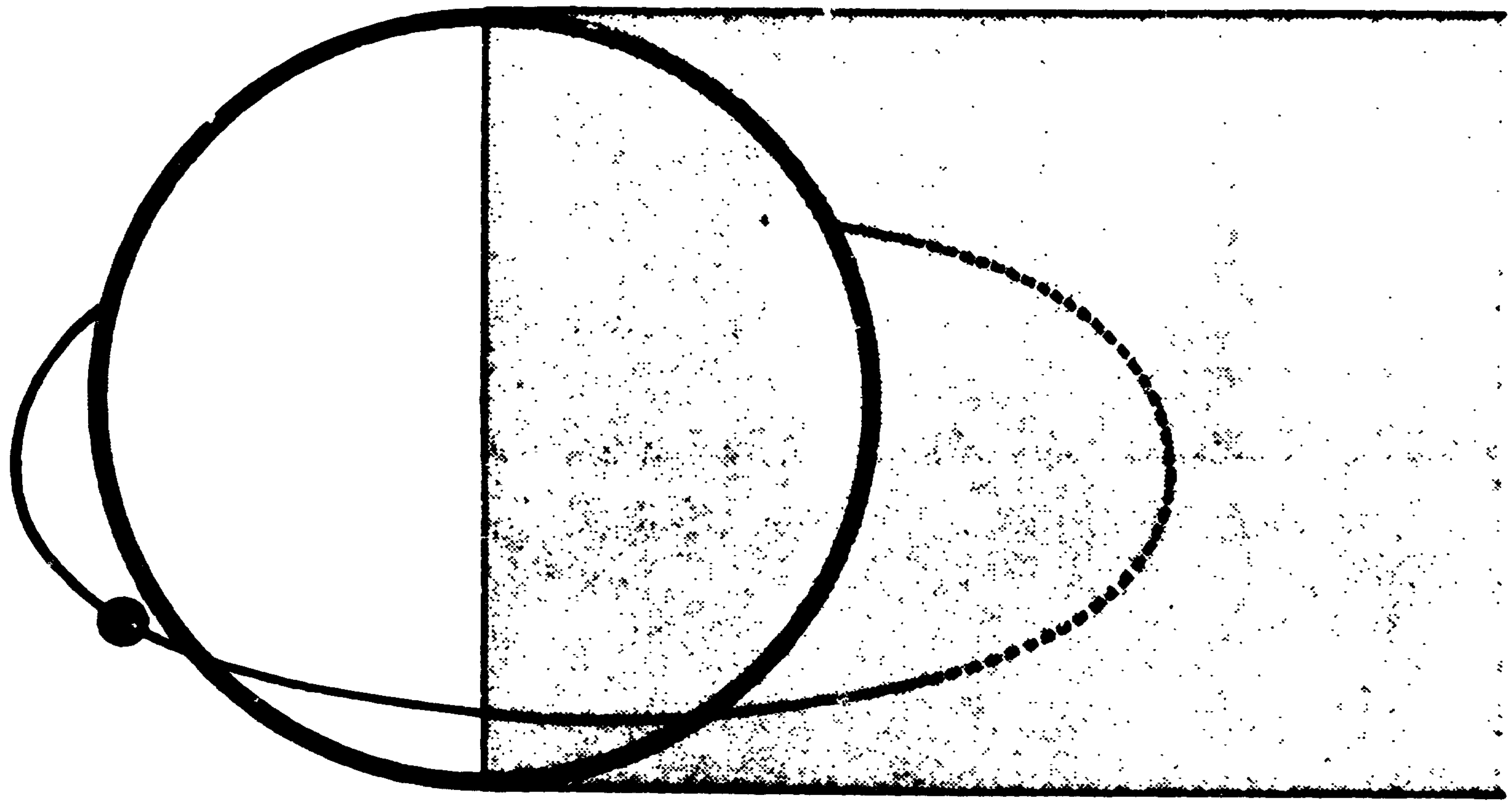

Satellite orbit showing passage through shadow.

Figure 8

Internal Temperatures and Per Cent Time Spent in Sunlight
Per Revolution for Explorer VII

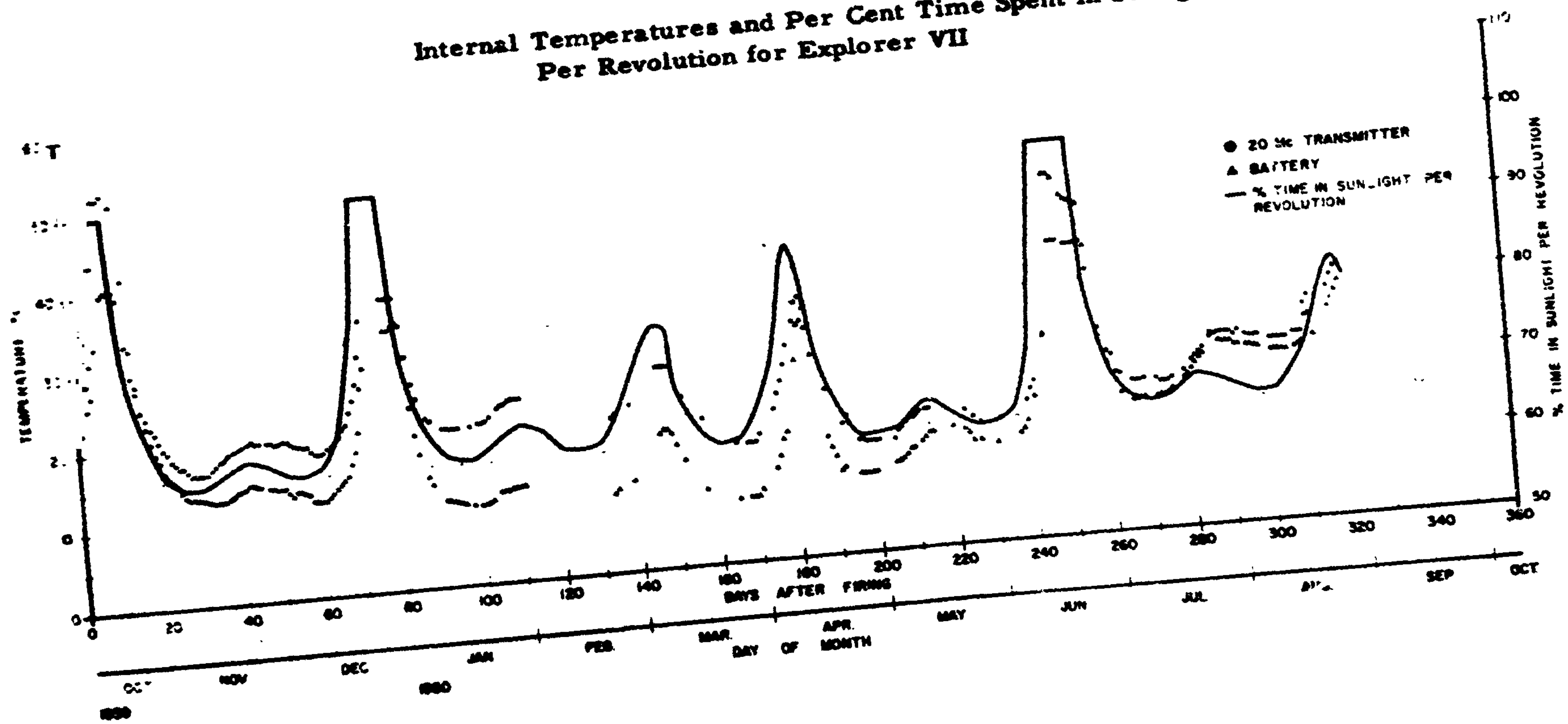

Figure 9

DATA INPUT FOR SHADOW-SUNLIGHT PROGRAM

1. Universal time during initial perigee passage
2. Number of days after vernal equinox
3. Eccentricity of orbit
4. Longitude of initial perigee
5. Latitude of initial perigee
6. Inclination of orbit
7. Altitude of perigee
8. North or South at initial perigee
9. Year

Figure 10

ALTERNATE FORM OF DATA INPUT

1. Anomalistic period
2. Argument of perigee
3. Longitude of ascending node
4. Inclination of orbit
5. Ratio of orbital semimajor axis to earth's radius
6. Time of ascending node crossing
7. Number of days after vernal equinox
8. Eccentricity of orbit
9. Year

Figure 11

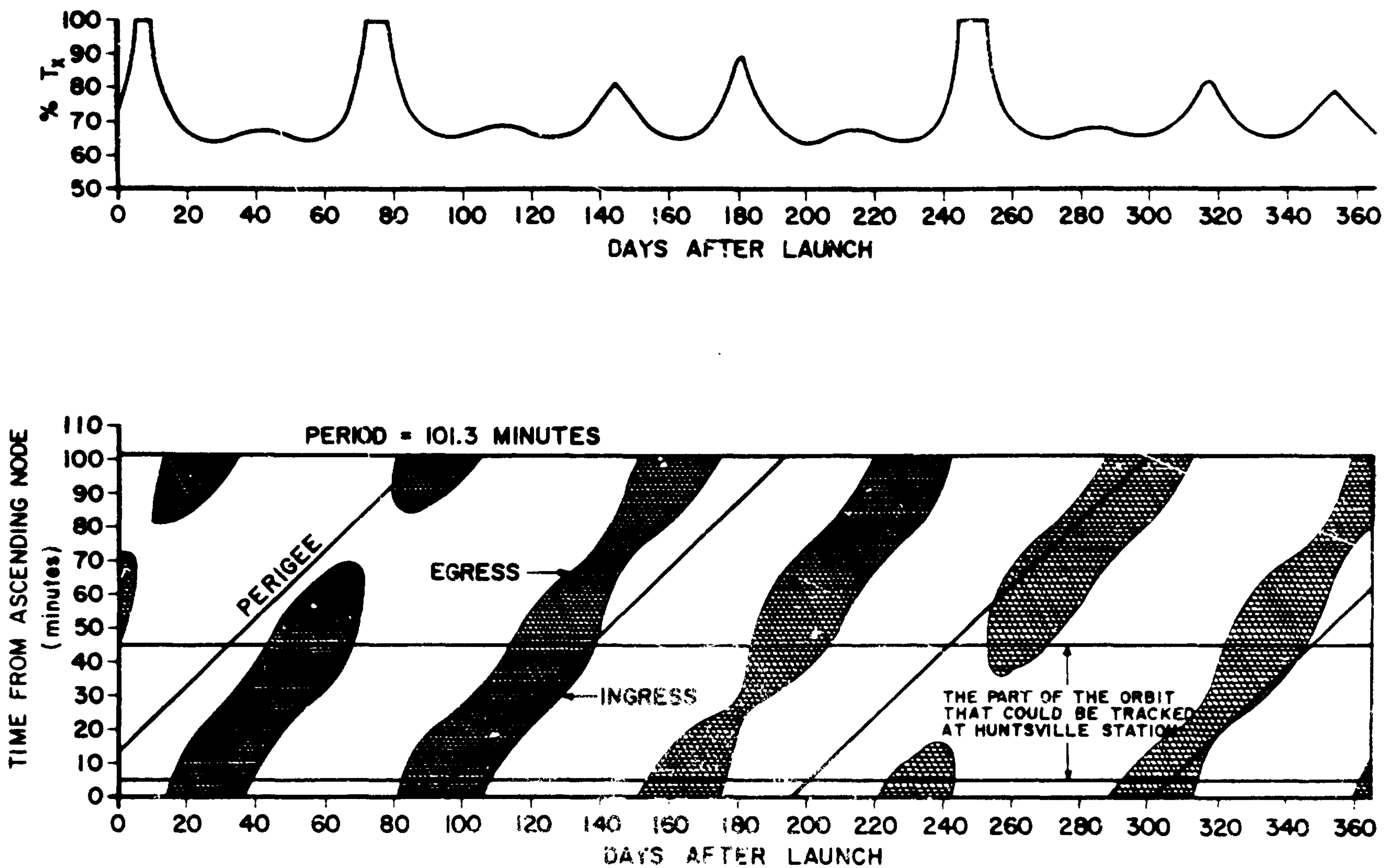

Results for EXPLORER VII (IOTA I)

Figure 12

Figure 11

BASIC EQUATIONS

$$\dot{T}_i H_i = \left\{A_{1i}\right\} \alpha_i S + \left\{A_{2i}\right\} \alpha_i B S$$

$$+ \left\{A_{3i}\right\} \epsilon_i E S - \left\{A_{4i}\right\} \epsilon_i \sigma T_i^4$$

$$+ \left\{Q_i\right\} + \sum_{j=1}^{n} \Big[C_{ij} (T_j - T_i) + R_{ij} (T_j^4 - T_i^4) \Big]$$

where $i = 1, 2, 3, \ldots, n$

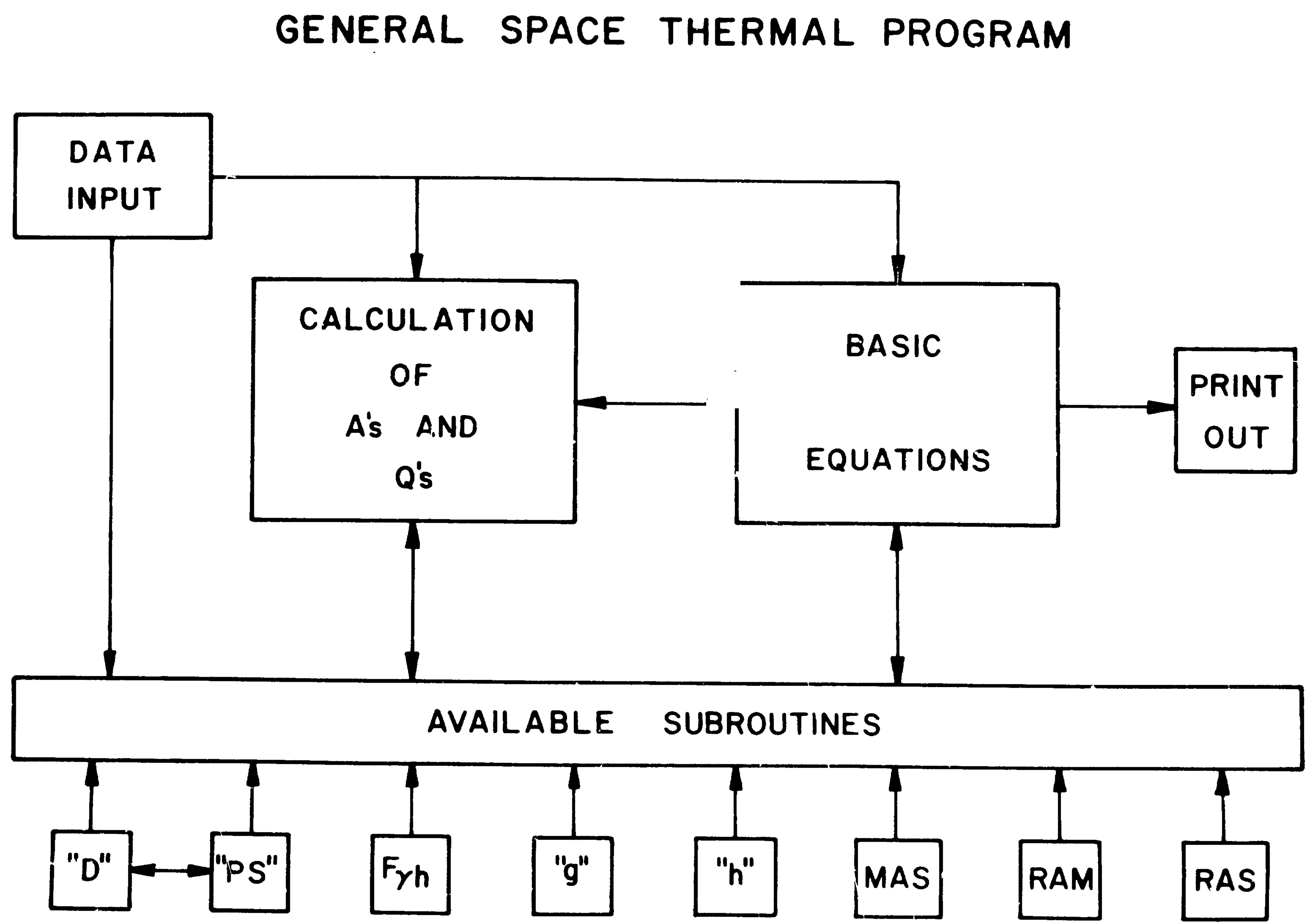

GENERAL SPACE THERMAL PROGRAM
DATA INPUT
CALCULATION OF A's AND Q's
BASIC EQUATIONS
PRINT OUT
AVAILABLE SUBROUTINES
"D"
"PS"
Fγh
"g"
"h"
MAS
RAM
RAS

Figure 15

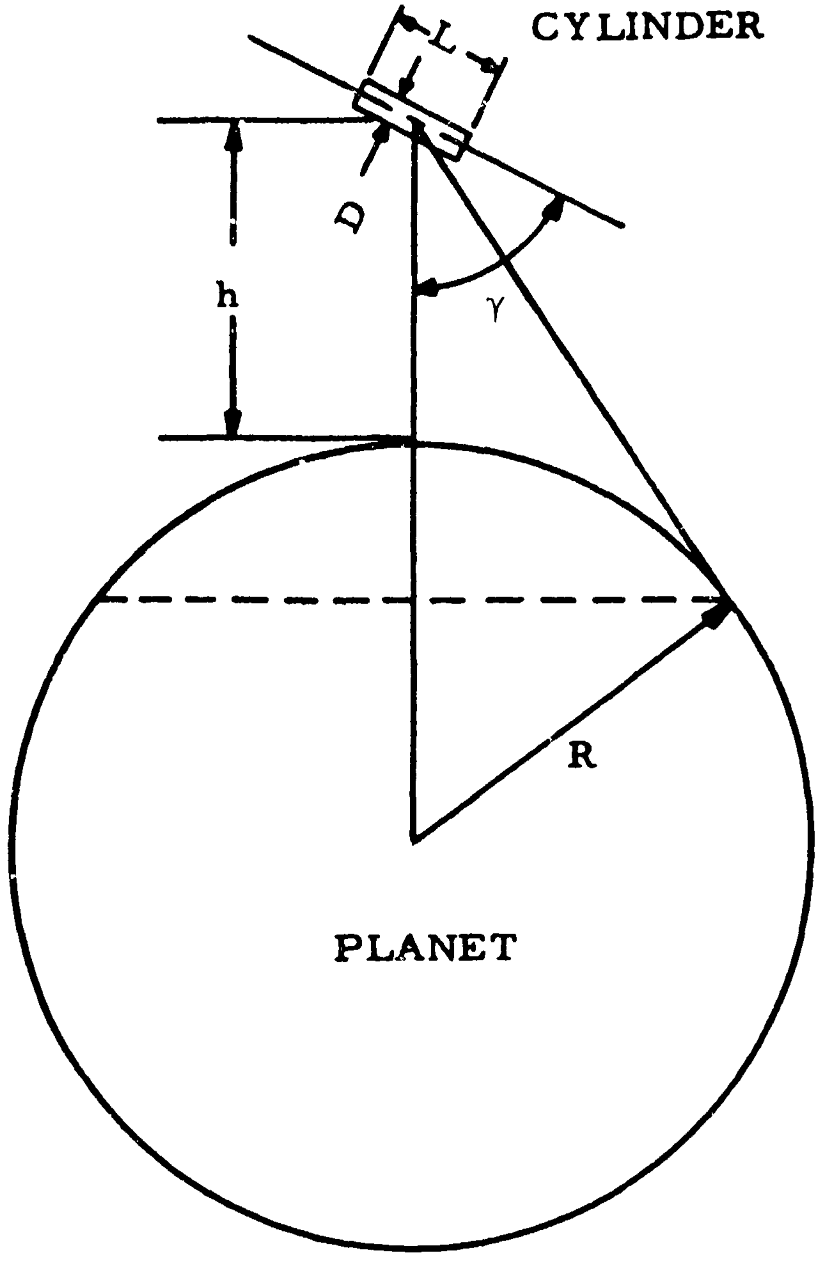

Geometry for Planetary Thermal Radiation to a Cylinder

Figure 16

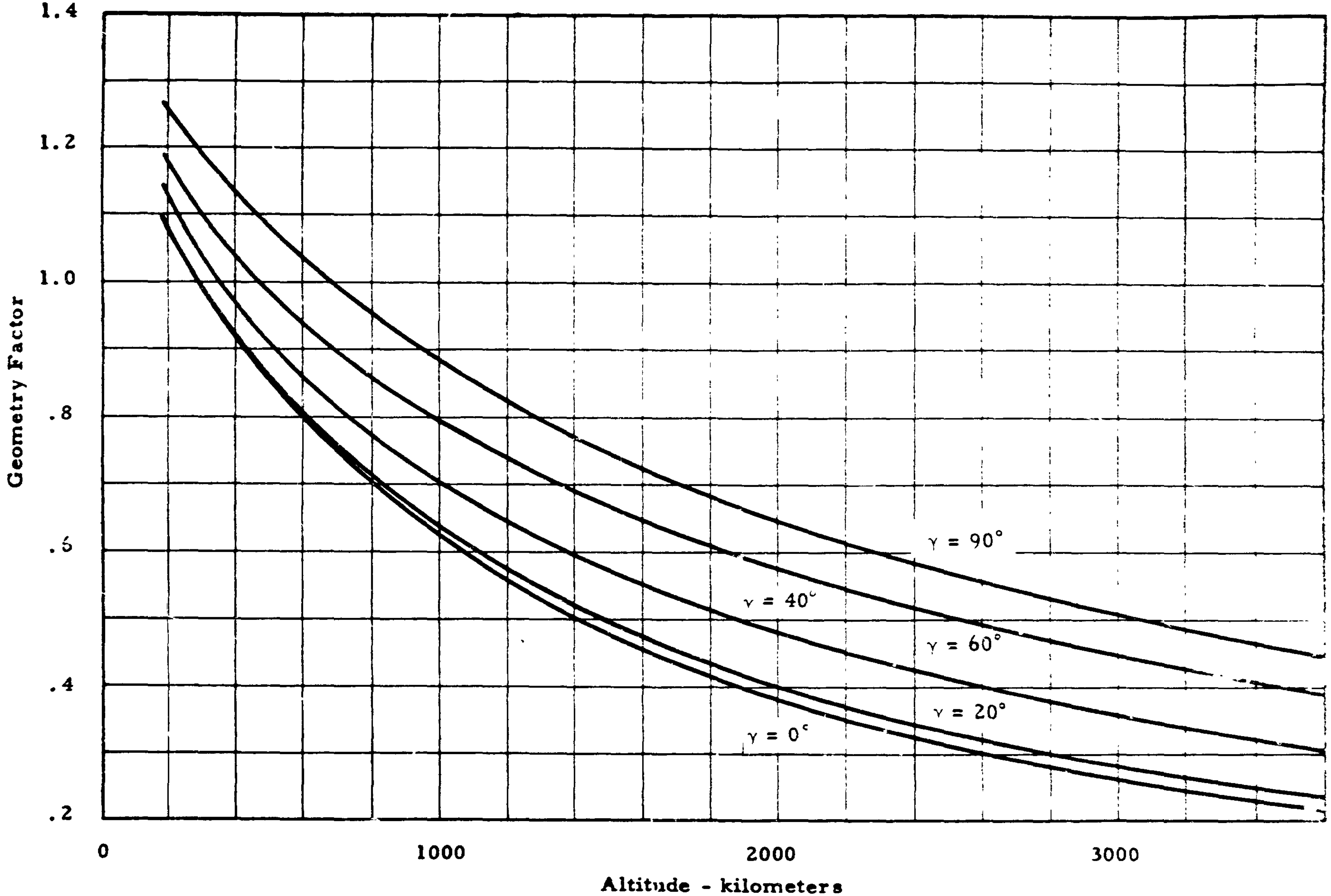

Geometry Factor vs. Altitude for
IR to a Cylinder

Figure 17

LEAST SQUARE CURVE FIT IN TWO VARIABLES

$$F_{\gamma, r} = \sum_{i=o}^{5} \left(\sum_{j=o}^{4} A_{ij} \gamma^{j} \right) h^{i}$$

Figure 18

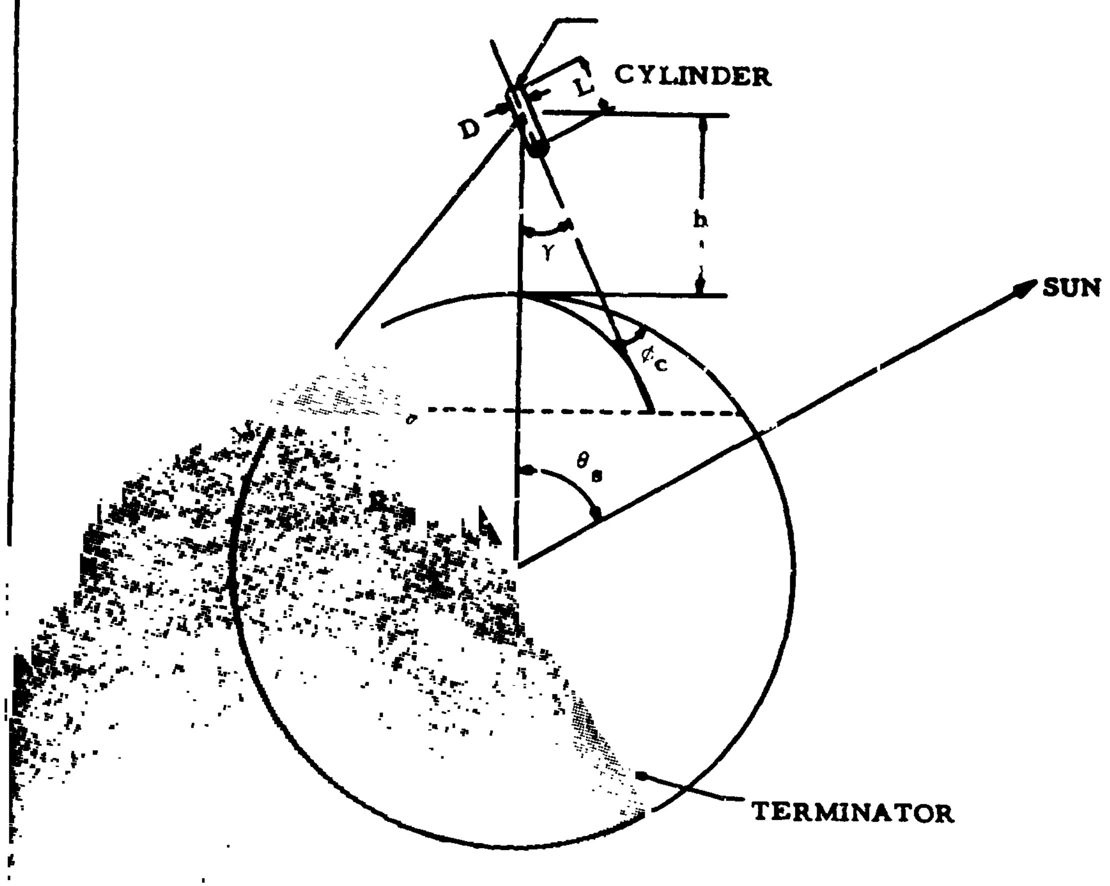

Geometry for Planetary Albedo
to a Cylinder

Figure 19

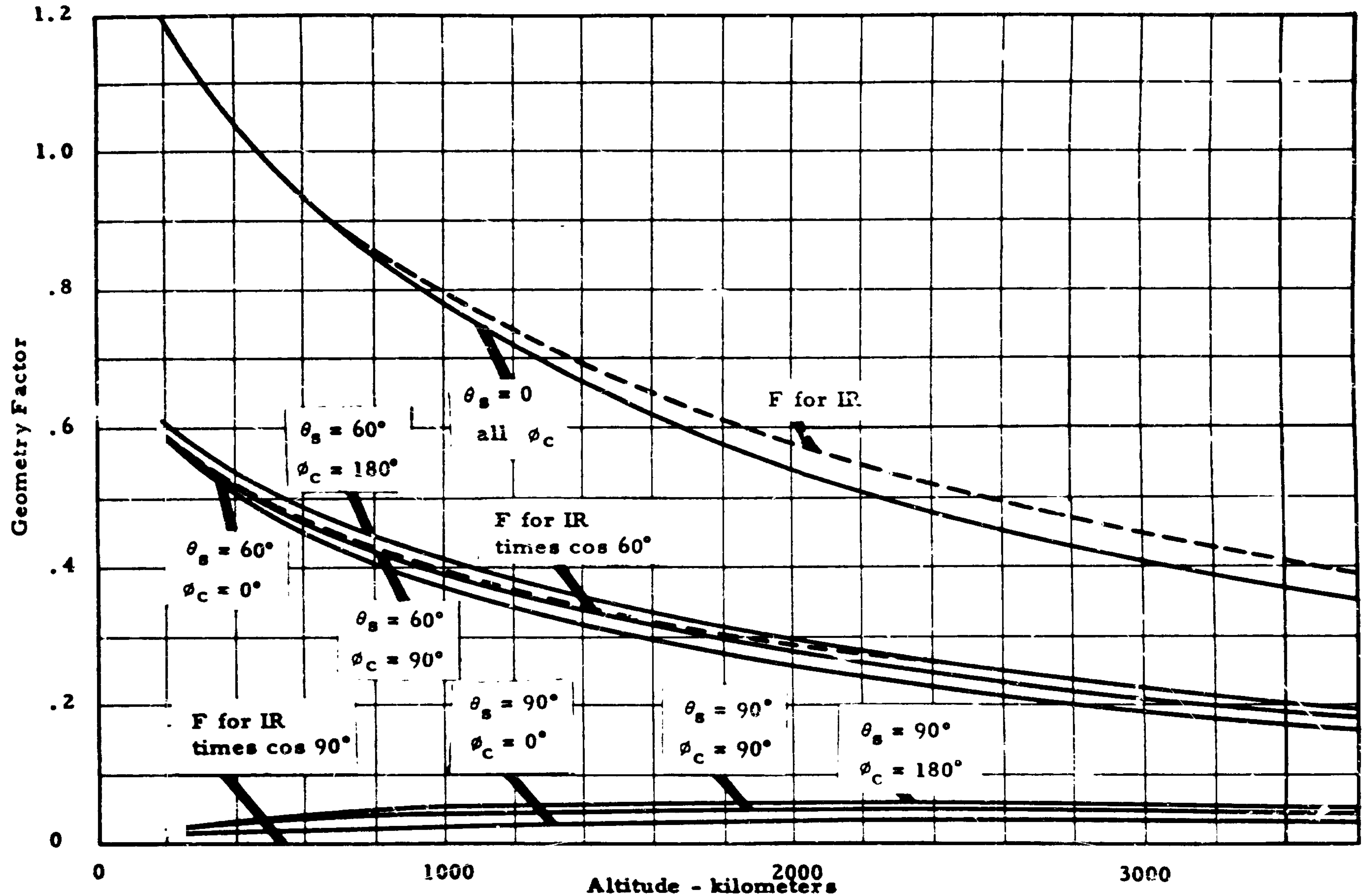

Geometry Factor vs. Altitude for Albedo to a Cylinder ($\gamma = 60°$)

Figure 20

NUMERICAL INTEGRATION BY KUTTA-SIMPSON ONE-THIRD RULE

$$T_{i\,new} = T_{i\,old} + \frac{1}{6}\left(\Delta^1 T_i + 2\,\Delta^2 T_i + 2\,\Delta^3 T_i + \Delta^4 T_i\right)$$

where

$$\Delta^1 T_i = \Delta t\ f\left(t_o,\ T_{io},\ T_{jo}\right)$$

$$\Delta^2 T_i = \Delta t\ f\left(t_o + \frac{1}{2}\Delta t,\ T_i + \frac{1}{2}\Delta^1 T_i,\ T_j + \frac{1}{2}\Delta^1 T_j\right)$$

$$\Delta^3 T_i = \Delta t\ f\left(t_o + \frac{1}{2}\Delta t,\ T_i + \frac{1}{2}\Delta^2 T_i,\ T_j + \frac{1}{2}\Delta^2 T_j\right)$$

$$\Delta^4 T_i = \Delta t\ f\left(t_o + \Delta t,\ T_i + \Delta^3 T_i,\ T_j + \Delta^3 T_j\right)$$

Figure 21

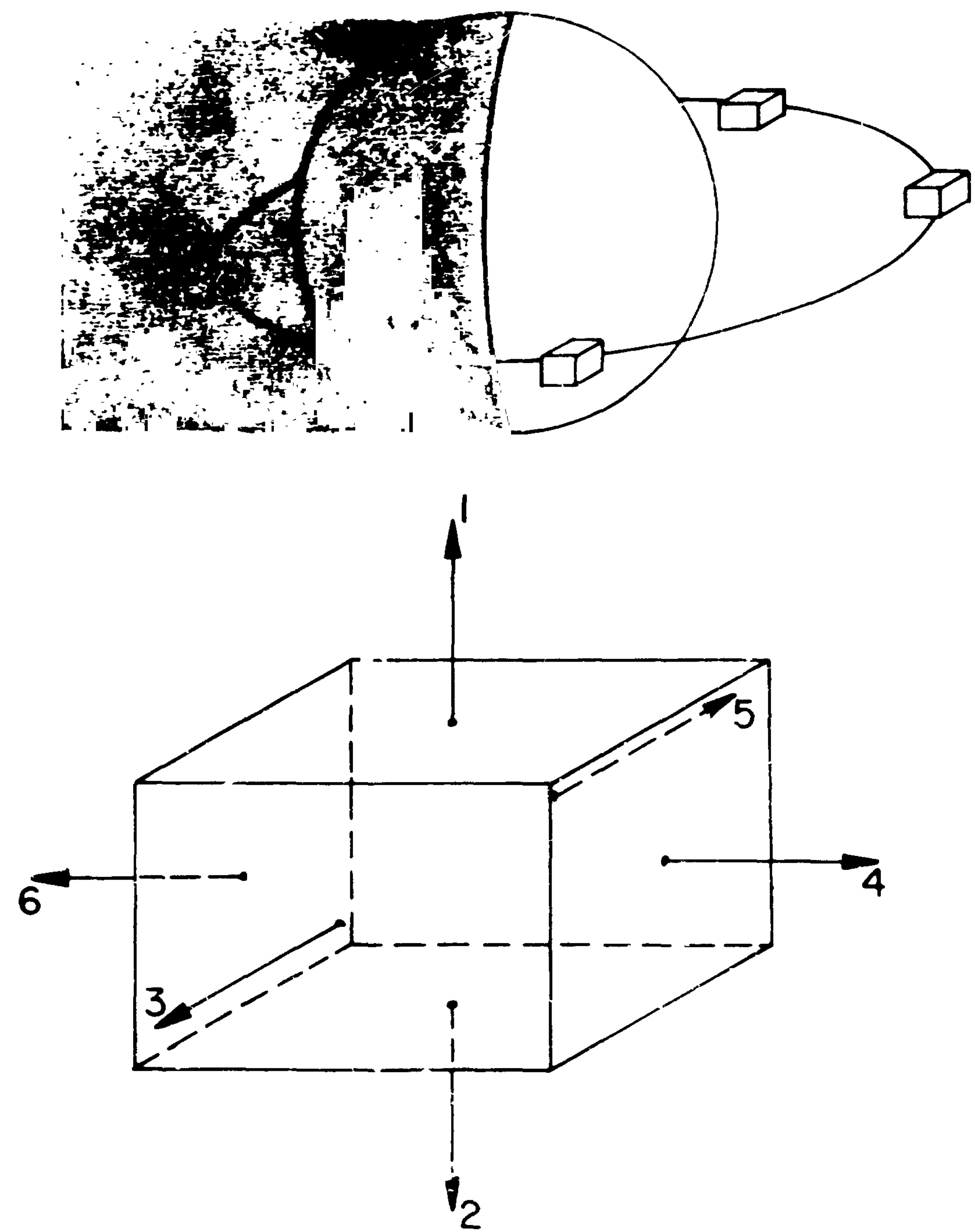

Figure [illegible]

INFORMATION NEEDED TO SET UP PROGRAM

$n = 6$

$A_{1i} = A_{4i} \cos (MAS)_i \; D$

$A_{2i} = A_{4i} F_{\gamma_i} h \cos (RAS)_i; \quad \gamma_i = 180^{\circ} - (RAM)_i$

$A_{3i} = A_{4i} F_{\gamma_i} h$

$A_{4i} = \text{Constant}$

$Q_i = 0$

$H_i = \text{Constant}$

Figure [illegible]

INPUT DATA NEEDED TO MAKE A RUN

$T_{io} = 300^\circ K$	$\gamma_{mi} = 0^\circ, 0^\circ, 0^\circ, 90^\circ, 180^\circ, 270^\circ$
$H_i = 1.13 \times 10^5$ Joules/$^\circ$K	$\delta_{mi} = +90^\circ, -90^\circ, 0^\circ, 0^\circ, 0^\circ, 0^\circ$
$\alpha_i = 0.80$	$a_S = 90^\circ$
$\epsilon_i = 0.55$	$\delta_S = 23.5^\circ$
$S = 1400$ watts/m²	$R_o = 6371$ km
$B = 0.39$	$R_p = 6671$ km
$E = 0.174$	$e = 0.1$
C_{ij} = see matrix	$T_x = 70^\circ$
R_{ij} = see matrix	$\Omega = 0^\circ$
$A_{4i} = 1\ m^2$	$i = 40^\circ$
$\sigma = 5.67 \times 10^{-8}$	$\omega = 120^\circ$

Figure 24

C_{ij}

i \ j	1	2	3	4	5	6
1	0	0	.76	.76	.76	.76
2	0	0	.76	.76	.76	.76
3	.76	.76	0	.76	0	.76
4	.76	.76	.76	0	.76	0
5	.76	.76	0	.76	0	.76
6	.76	.76	.76	0	.76	0

$R_{ij} \times 10^{-8}$

i \ j	1	2	3	4	5	6
1	0	1.245	1.150	1.150	1.150	1.150
2	1.245	0	1.150	1.150	1.150	1.150
3	1.150	1.150	0	1.150	1.245	1.150
4	1.150	1.150	1.150	0	1.150	1.245
5	1.150	1.150	1.245	1.150	0	1.150
6	1.150	1.150	1.150	1.245	1.150	0

Figure 25

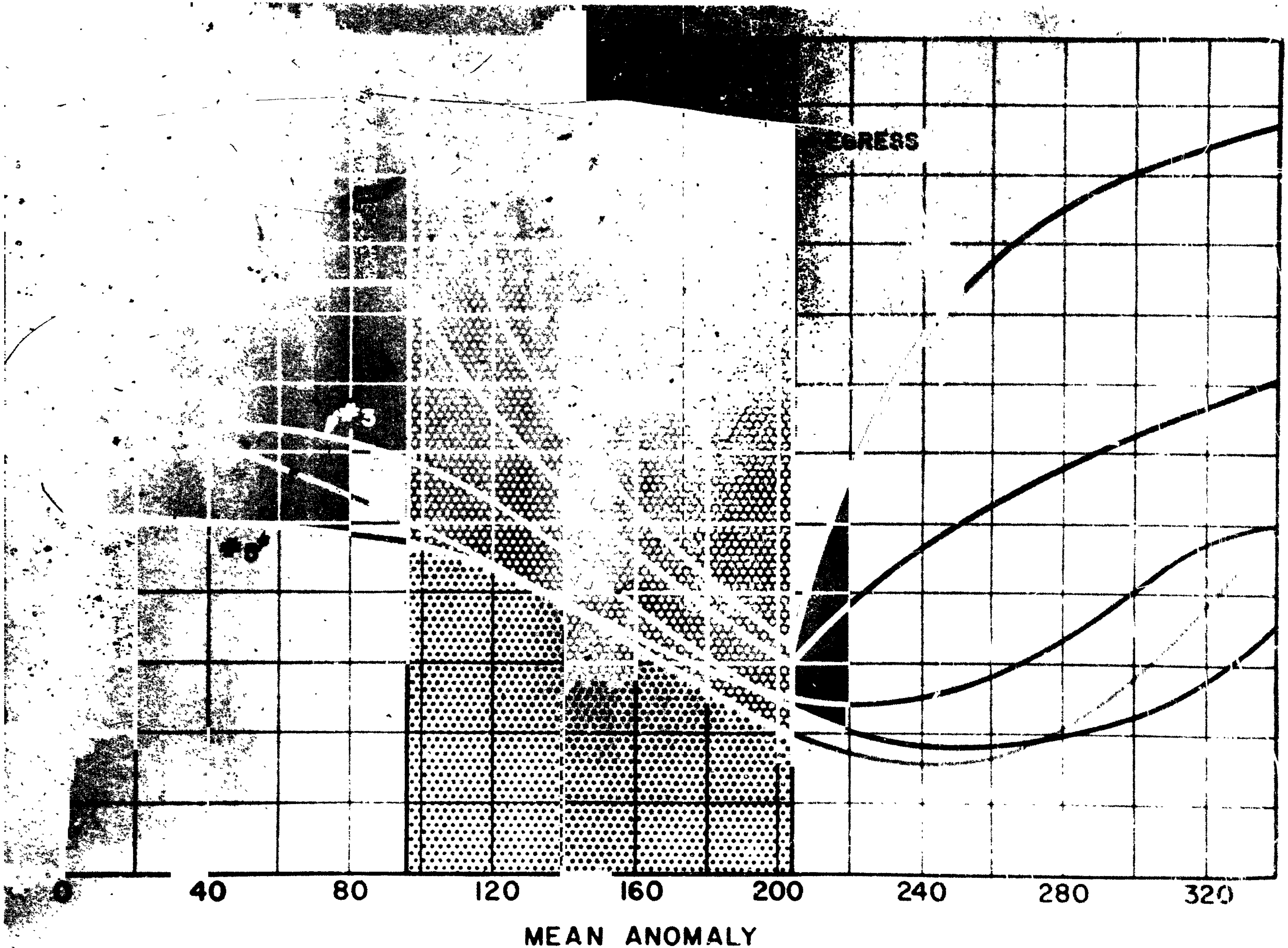

Figure 26

SATELLITE HEAT TRANSFER PROGRAMS

by

Edward I. Powers
NASA Goddard Space Flight Center
Greenbelt, Maryland

Computer Programs for Spacecraft Thermal Design at Goddard Space Flight Center

The thermal design of an earth satellite requires an accurate knowledge of both thermal radiation inputs and internal temperature distribution. The use of the IBM-7094 as an analytical tool to determine these functions is now widely employed.

At Goddard Space Flight Center, two programs are used extensively. One determines the thermal radiation (i.e., direct solar radiation, earth emitted radiation, and albedo) to a spinning flat plate. The program is geared toward the analysis of spin-stabilized spacecraft, but can be applied to non-spinning plates either earth or space oriented. The second program determines the temperature distribution and net heat flow, provided the appropriate conductances, radiation view factors, and thermal properties are known.

A detailed discussion of these programs is presented below.

THERMAL RADIATION TO A FLAT SURFACE ROTATING ABOUT AN ARBITRARY AXIS IN AN ELLIPTICAL EARTH ORBIT: APPLICATION TO SPIN-STABILIZED SATELLITES

N64-17745

by
Edward I. Powers
Goddard Space Flight Center

SUMMARY

The derivation of total thermal radiation incident upon a flat plate rotating about an arbitrary axis is presented. The functional relationships between position in an elliptical earth orbit and direct solar radiation, earth-reflected solar radiation (albedo), and earth-emitted radiation (earthshine) are included. The equations have been programmed for the IBM 7090 digital computer, resulting in solutions which relate the incident radiation to spin axis orientation and orbital position. Several representative orbits for a typical geometrical configuration were analyzed and are presented as examples.

CONTENTS

THERMAL RADIATION TO A FLAT SURFACE ROTATING ABOUT AN ARBITRARY AXIS IN AN ELLIPTICAL EARTH ORBIT: APPLICATION TO SPIN-STABILIZED SATELLITES

by
Edward I. Powers
Goddard Space Flight Center

INTRODUCTION

The satisfactory operation of an artificial satellite depends upon maintaining the payload temperature within prescribed limits. For example, the standard batteries employed in present-day spacecraft generally restrict the temperature limits to 0° and 40°C. Often experiments located within the satellite structure further restrict this variation.

The temperature level of a satellite may be determined by solving the instantaneous energy balance

$$P + S\alpha_s A_p + q_{alb} + q_{es} = \sigma\epsilon A_s T^4 + WC_p \frac{dT}{dt} ,$$

where

P = internal power dissipation,

S = solar constant,

α_s = solar absorptance,

A_p = instantaneous projected area for sunlight,

q_{alb} = reflected solar radiation (albedo),

q_{es} = earth-emitted radiation (earthshine),

σ = Stefan-Boltzmann constant,

ϵ = infrared emittance,

A_s = total surface area,

$\bar{T}^4$ = mean fourth power, surface temperature,

WC_p = heat capacity of the satellite,

$\frac{dT}{dt}$ = time rate of change of satellite temperature.

If the average orbital temperature is being computed, the last term is dropped. In this case al. heat input terms represent integrated orbital values.

It should be noted that the above equation, as a representation of the entire satellite, is greatly oversimplified. The values for ϵ and α_s generally vary over the surface and great fluctuations in skin temperature may exist. In practice the thermal analysis consists of the development of a thermal model which represents a fine mesh of interconnected isothermal nodes. The appropriate relationship between nodes in regard to thermal conduction and radiation interchange must be established.

The energy balance for each node of a thermal model may be written

$$P_n + S\alpha_{s_n} A_{p_n} + q_{alb_n} + q_{es_n} + \sum_m C_{nm}\left(T_m - T_n\right) + \sigma \sum_m E_{nm} F_{nm}\left(T_m^4 - T_n^4\right) = \sigma \epsilon A_{s_n} T_n^4 + \left(WC_p\right)_n \frac{dT_n}{dt} ,$$

where

C_{nm} = conductance between nodes n and m,

E_{nm} = effective emissivity between nodes n and m,

F_{nm} = shape factor-area product between nodes n and m.

Since the major interest at present is to determine the satellite temperature level and not the gradients within, a discussion of the terms in the first equation is in order.

For most passive controlled satellites P is relatively small compared with the total radiation input and does not have a significant effect on the satellite mean temperature. The magnitude of this effect, however, depends upon the ϵ of the surface (e.g. a surface with a low absolute ϵ may raise the internal temperature significantly because the skin has a limited capacity for re-radiation).

The remaining three heat sources, direct solar heating, earth-reflected solar heating (albedo), and earth-emitted radiation (earthshine), represent the significant inputs to the satellite. It is apparent that an adequate thermal design is predicated upon a reasonably accurate knowledge of these thermal radiation inputs. The major source of energy—direct solar radiation—is fortunately the most accurately obtained. Since the sun's rays impinging upon the satellite are virtually parallel, the problem is simply one of determining the instantaneous orientation of each external face with respect to the solar vector.

The calculation of earthshine is considerably less precise, requiring fundamental assumptions to reduce the complexity of computation. These include the assumptions that the earth is a diffusely emitting blackbody and that the surface temperature is uniform at 450°R. This permits direct calculation of energy input from all visible positions on the earth. Since all locations supply varying inputs, an integral equation must be solved to obtain the total incident energy.

The albedo determination involves a similar integration. The earth in this case is assumed to be a diffusely reflecting sphere. In addition, the source intensity is a function of the satellite location relative to the sunlit portion of the earth.

For a nonrotating satellite whose orientation is "fixed in space" the calculation of the thermal radiation fluxes is performed at any interval during the orbit. At each orbital position a particular flat surface may or may not "see" the entire part of the earth's cap visible from the satellite. In the latter case integration for albedo and earthshine must exclude the shaded portion of the cap. Spin-stabilized satellites which rotate uniformly about the spin axis greatly complicate the analysis. The rotation around an arbitrary axis means in general that the heat fluxes vary, since the visible portion of the earth is a function of this rotation.

The analysis presented herein is based upon the energy impinging upon a flat surface whose orientation is defined in vector notation (by the normal vector), and which is rotating about an arbitrary axis. This has a much broader application than may be realized at first. Although the obvious application is for spin-stabilized satellites, the results apply to any body of revolution. Here the interest lies in the variation of flux about the axis rather than an average value per spin. Thus, with the orientation of a single flat plate, the impinging fluxes on cylinders and cones are obtained. A sphere or a shape with a variable surface curvature along its axis requires several or many such plates, depending upon the precision required. It can be seen that the thermal radiation to the entire satellite surface may be found by simply considering a handful of appropriately oriented flat plates.

The purpose of this paper is to present, in general form, the derivation of the governing equations for the radiation energy sources as stated. The equations refer specifically to a flat surface rotating about an axis whose orientation is arbitrary. The dependence upon orbital position is included; the results of the numerical integration of these equations, encompassing a suitable range of applicable orbits, is presented.

COORDINATE SYSTEMS AND VECTOR REPRESENTATION

The primary coordinate system is fixed with respect to the orbit (Figure 1). The XY plane lies in the plane of the orbit with the X axis coincident with the line connecting the center of the earth (the focus of the ellipse) and perigee.

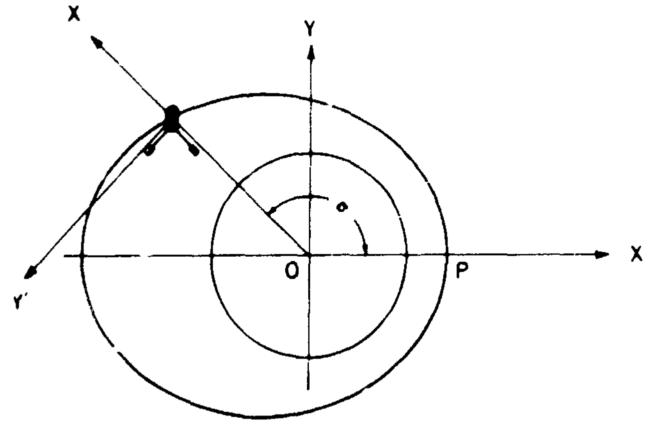

LEGEND
O - EARTH CENTER
P - PERIGEE

Figure 1—Coordinate systems.

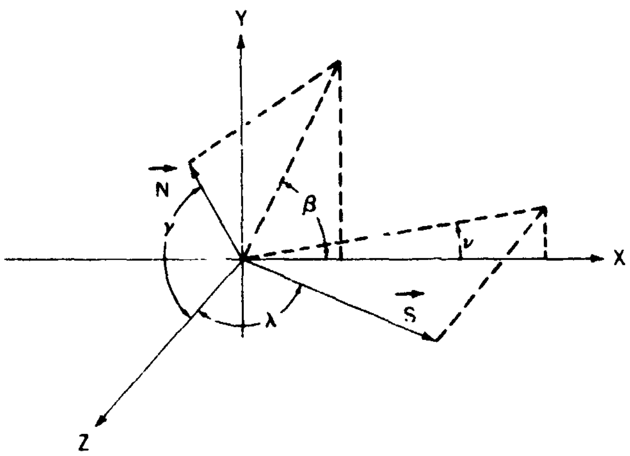

Figure 2—Orientation of normal and solar vectors.

As the satellite traverses the orbit, the instantaneous location is defined by the angle α. The altitude, therefore, may be determined at any instant by

$$A(\alpha) = \frac{(P + R_e)(1 + e)}{1 + e \cos \alpha} - R_e \tag{1}$$

where

$A(\alpha)$ = altitude,

P = altitude at perigee,

R_e = radius of the earth,

e = eccentricity of the orbit.

The orientation of the unit vectors (Figure 2) representing the normals to the flat plates, N, and the solar vector, S, are specified by the following angles:

β = angle between the projection of N on the XY plane and the X axis,

γ = angle between N and the Z axis,

ν = angle between the projection of S on the XY plane and the X axis,

λ = angle between S and the Z axis.

The vectorial representations in the fixed coordinate system are thus

$$\mathbf{N} = \cos\beta \sin\gamma \, \mathbf{i} + \sin\beta \sin\gamma \, \mathbf{j} + \cos\gamma \, \mathbf{k} \tag{2}$$

and

$$\mathbf{S} = \cos\nu \sin\lambda \, \mathbf{i} + \sin\nu \sin\lambda \, \mathbf{j} + \cos\lambda \, \mathbf{k} \; . \tag{3}$$

It is convenient to introduce an instantaneous coordinate system (X′ Y′ Z′) whose origin is fixed in the satellite (Figure 1). The X′Y′ plane lies in the orbital plane with the X′ axis coincident with the line from the earth's center to the satellite. Z′ and Z have the same orientation.

The vectors N and S in the primed system are

$$\mathbf{N} = \cos(\beta - \alpha) \sin\gamma \, \mathbf{i}' + \sin(\beta - \alpha) \sin\gamma \, \mathbf{j}' + \cos\gamma \, \mathbf{k}' \; , \tag{4}$$

$$\mathbf{S} = \cos(\nu - \alpha) \sin\lambda \, \mathbf{i}' + \sin(\nu - \alpha) \sin\lambda \, \mathbf{j}' + \cos\lambda \, \mathbf{k}' \; . \tag{5}$$

In a similar manner the expression for the spin axis vector **A** may be shown to be

$$\mathbf{A} = \cos(\delta - \alpha) \sin\mu \; \mathbf{i}' + \sin(\delta - \alpha) \sin\mu \; \mathbf{j}' + \cos\mu \; \mathbf{k}' \tag{6}$$

where

δ = angle between the projection of **A** on the XY plane and the X axis,

μ = angle between **A** and the Z axis.

PLATE ROTATING ABOUT THE SPIN AXIS

For spin-stabilized satellites the normal vectors **N**, which represent the orientation of the exterior surfaces, rotate about the spin axis. In determining both instantaneous and average heat fluxes, the orientation of **N** as a function of this rotation with respect to the primed coordinate system $(X'\,Y'\,Z')$ must be known. This is accomplished by defining a third coordinate system $X''\,Y''\,Z''$ (Figure 3). The X'' axis is coincident with the spin axis **A**. Y'' is defined so that it lies in the plane formed by X'' and an arbitrary fixed position of the normal vector $\mathbf{N}_o$.*

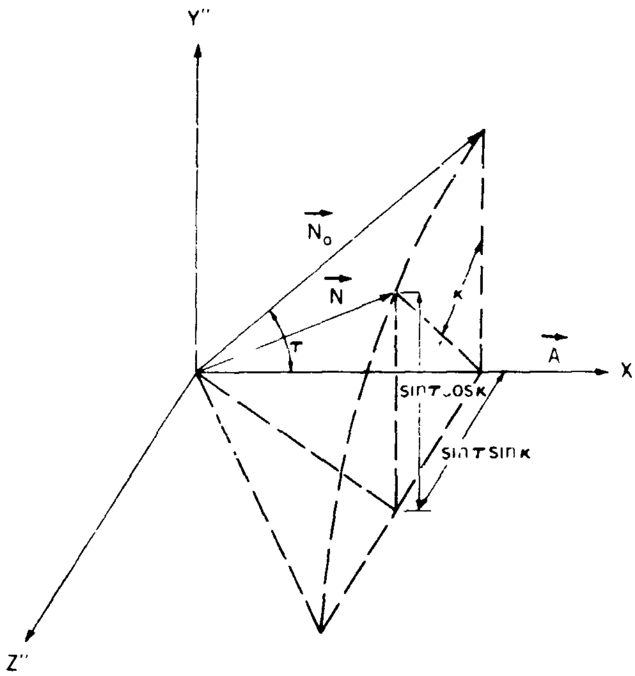

Figure 3—Double-primed coordinate system.

In Figure 3, the following terms may be evaluated:

$$\cos\tau = \cos(\beta - \alpha) \sin\gamma \cos(\delta - \alpha) \sin\mu$$
$$+ \sin(\beta - \alpha) \sin\gamma \sin(\delta - \alpha) \sin\mu + \cos\gamma \cos\mu \,, \tag{7}$$

$$\sin\tau = \sqrt{1 - \cos^2\tau} \,,$$

$$\mathbf{N} = \cos\tau \; \mathbf{i}'' + \sin\tau \cos\kappa \; \mathbf{j}'' + \sin\tau \sin\kappa \; \mathbf{k}'' \tag{8}$$

It can be seen that the angle between the spin axis and $\mathbf{N}_o$ can be computed only in the first and second quadrants of the $X''Y''$ plane. This has little effect since κ varies from 0 to 2π (a rotation). [If the vector $\mathbf{N}_o$ lies in the third quadrant (of the $X''Y''$ plane) the initial position for rotation remains in the second quadrant.] The objective now is to relate the double-primed unit vectors to the primed vectors in order to determine **N** in the primed system.

*Since a complete rotation occurs, the orientation of $\mathbf{N}_o$ merely indicates the starting point.

The projections of j″ and k″ in the primed coordinate system are found in the following manner: The value for the unit vector k″ is

$$\mathbf{k}'' = \frac{\mathbf{A} \times \mathbf{N}_o}{|\mathbf{A} \times \mathbf{N}_o|} = \frac{g\mathbf{i}' + h\mathbf{j}' + l\mathbf{k}'}{\sqrt{g^2 + h^2 + l^2}} , \tag{9}$$

where

$$g = \sin(\delta - \alpha)\sin\mu\cos\gamma - \cos\mu\sin(\beta - \alpha)\sin\gamma ,$$

$$h = \cos\mu\cos(\beta - \alpha)\sin\gamma - \cos(\delta - \alpha)\sin\mu\cos\gamma ,$$

$$l = \cos(\delta - \alpha)\sin\mu\sin(\beta - \alpha)\sin\gamma$$

$$- \sin(\delta - \alpha)\sin\mu\cos(\beta - \alpha)\sin\gamma$$

similarly

$$\mathbf{j}'' = \frac{(\mathbf{A} \times \mathbf{N}_o) \times \mathbf{A}}{|(\mathbf{A} \times \mathbf{N}_o) \times \mathbf{A}|} = \frac{m\mathbf{i}' + n\mathbf{j}' + o\mathbf{k}'}{\sqrt{m^2 + n^2 + o^2}} \tag{10}$$

where

$$m = h\cos\mu - l\sin(\delta - \alpha)\sin\mu ,$$

$$n = l\cos(\delta - \alpha)\sin\mu - g\cos\mu ,$$

$$o = g\sin(\delta - \alpha)\sin\mu - h\cos(\delta - \alpha)\sin\mu .$$

N may now be determined in the primed coordinate system (X′ Y′ Z′). By rewriting the double-primed unit vectors,

$$\left.\begin{aligned} \mathbf{i}'' &= p\mathbf{i}' + q\mathbf{j}' + r\mathbf{k}' \\ \mathbf{j}'' &= s\mathbf{i}' + t\mathbf{j}' + u\mathbf{k}' \\ \mathbf{k}'' &= v\mathbf{i}' + w\mathbf{j}' + x\mathbf{k}' \end{aligned}\right\} . \tag{11}$$

where

$$p = \cos(\delta - \alpha)\sin\mu ,$$

$$q = \sin(\delta - \alpha)\sin\mu ,$$

$$r = \cos\mu ,$$

$$s = \frac{m}{\sqrt{m^2 + n^2 + o^2}} ,$$

$$t = \frac{n}{\sqrt{m^2 + n^2 + o^2}} ,$$

$$u = \frac{o}{\sqrt{m^2 + n^2 + o^2}} ,$$

$$v = \frac{g}{\sqrt{g^2 + h^2 + l^2}} ,$$

$$w = \frac{h}{\sqrt{g^2 + h^2 + l^2}} ,$$

$$x = \frac{l}{\sqrt{g^2 + h^2 + l^2}} .$$

By substituting for i'', j'', and k'' in Equation 8

$$N = ai' + bj' + ck' , \qquad (12)$$

where

$$a = p\cos\tau + s\sin\tau\cos\kappa + v\sin\tau\sin\kappa ,$$

$$b = q\cos\tau + t\sin\tau\cos\kappa + w\sin\tau\sin\kappa ,$$

$$c = r\cos\tau + u\sin\tau\cos\kappa + x\sin\tau\sin\kappa ,$$

where κ is the angle of rotation. N may now be evaluated at any position during rotation throughout the orbit in the primed system (X' Y' Z').

DETERMINATION OF EARTHSHINE

The general expression for the radiation intensity dq, from a diffusely emitting source dA_e, impinging upon a unit area, is as follows:

$$dq = \frac{I\cos\omega\cos\eta\, dA_e}{D^2} , \qquad (13)$$

where

I = source intensity,

ω = angle between the line connecting the unit area with dA_e and the normal to dA_e (N_e),

η = angle between the line connecting dA_e with the unit area and the normal to the unit area,

D = distance between the unit area and dA_e.

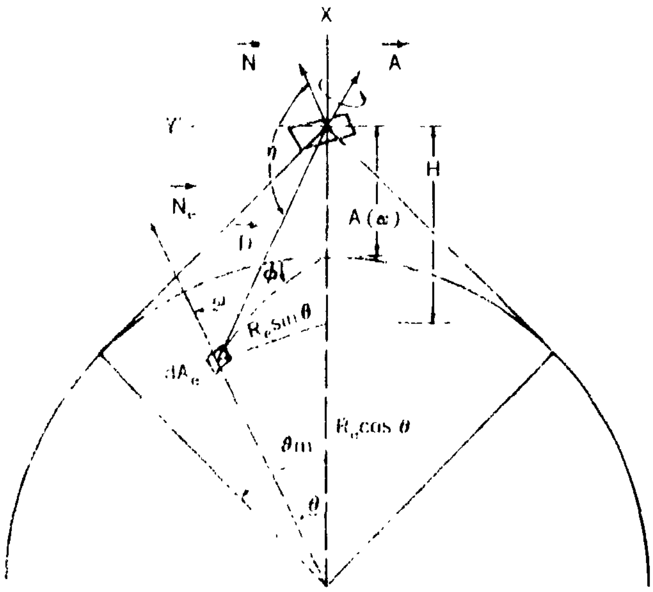

Figure 4—Earth's cap visible from satellite (ϕ = 0 when coincident with γ').

With the application of this equation to a flat plate of unit area at an altitude $A(\alpha)$, the radiation intensity impinging upon the plate is

$$q_E = \frac{\sigma T_e^4}{\pi} \int_0^{\theta_m} \int_0^{2\pi} \frac{\cos\omega \cos\eta \, dA_e}{D^2} \tag{14}$$

where

- σ = Stefan-Boltzmann constant,
- T_e = mean black body temperature of the earth's surface,
- σT_e^4 = the heat flux leaving the source dA_e.

From the geometry of Figure 4 (which is similar to a sketch used by Katz*) and the vector notation presented, the terms in the equation may be defined more specifically:

$$\mathbf{D} = H\mathbf{i}' + R_e \sin\theta \cos\phi \, \mathbf{j}' + R_e \sin\theta \sin\phi \, \mathbf{k}' ,$$

$$= \left[A(\alpha) + R_e (1 - \cos\theta)\right] \mathbf{i}' + R_e \sin\theta \cos\phi \, \mathbf{j}' + R_e \sin\theta \sin\phi \, \mathbf{k}' ,$$

$$D^2 = \left[A(\alpha) + R_e (1 - \cos\theta)\right]^2 + R_e^2 \sin^2\theta ,$$

$$\omega = \theta + \tan^{-1}\left[\frac{R_e \sin\theta}{A(\alpha) + R_e (1 - \cos\theta)}\right] ,$$

$$\cos\eta = \frac{\mathbf{D} \cdot \mathbf{N}}{|\mathbf{D}|} ,$$

$$= \left\{ a\left[A(\alpha) + R_e (1 - \cos\theta)\right] + b R_e \sin\theta \cos\phi + c R_e \sin\theta \sin\phi \right\} \cdot \frac{1}{\sqrt{\left[A(\alpha) + R_e (1 - \cos\theta)\right]^2 + \left(R_e^2 \sin^2\theta\right)}} ,$$

$$\theta_m = \cos^{-1}\left[\frac{R_e}{A(\alpha) + R_e}\right] .$$

*Katz, A. J., "Determination of Thermal Radiation Incident upon the Surfaces of an Earth Satellite in an Elliptical Orbit," Grumman Aircraft Engineering Corp., Rept. XP 12.20, May 1960.

Equation 14 may now be written in the form

$$q_E = \frac{\sigma T_e^4}{\pi} \int_0^{\cos^{-1}\left[\frac{R_e}{A(\alpha) + R_e}\right]} \int_0^{2\pi} \cos\left\{\theta + \tan^{-1}\left[\frac{R_e \sin\theta}{A(\alpha) + R_e (1-\cos\theta)}\right]\right\} \cdot$$

$$\cdot \left\{a\left[- A(\alpha) + R_e (1-\cos\theta)\right] + b R_e \sin\theta \cos\phi + c R_e \sin\theta \sin\phi\right\} \cdot$$

$$\cdot \left\{\frac{1}{\left[A(\alpha) + R_e (1-\cos\theta)\right]^2 + R_e^2 \sin^2\theta}\right\}^{3/2} R_e^2 \sin\theta \, d\phi \, d\theta \; . \tag{15}$$

The limits of integration are such that the part of the earth cap visible from the instantaneous location of the satellite is included. For most practical cases, at least a portion of the cap is not visible from a plate because of its orientation. Attempts to define the appropriate integration limits for such cases are extremely laborious. Since the equations cannot be solved without the aid of a high speed computer, an alternative approach is employed.* The numerical integration includr the entire visible part of the earth cap as stated, but the contributions of the elemental area that the plate does not see are deleted if the local value of $\cos\eta$ is negative.

Equation 15 represents the flux for the instantaneous orientation of the plate. Interest also lies in the determination of the flux for a complete rotation of the plate about the satellite spin axis. The average value for q_E is therefore

$$q_{E_{av.}} = \frac{1}{2\pi} \int_0^{2\pi} q_E \, d\kappa \tag{16}$$

where κ is the rotational angle.

DETERMINATION OF ALBEDO

The calculation for the albedo input to an orbiting plate is similar to that for the earthshine but involves additional basic assumptions. The reflectance of the earth depends on what is the visible surface—land, water, snow, cloud cover, etc. Until precise data is available which indicates the functional relationship between the albedo and the visible surface, an approximate mean value of 35 percent appears satisfactory.

The reflected radiation is assumed to be diffuse. The local earth-reflected intensity varies with the cosine of the angle between the solar vector and the local normal. Since the input to the plate is a function of the source intensity of the visible elemental areas, the reflected radiation can be expressed by

*Katz, A. J., op. cit.

$$q_A = \frac{S\ alb}{\pi} \int_0^{\cos^{-1}\left[\frac{R_e}{A(\alpha)+R_e}\right]} \int_0^{2\pi} \cos\left\{\theta + \tan^{-1}\left[\frac{R_e \sin\theta}{A(\alpha) + R_e(1-\cos\theta)}\right]\right\} \cdot$$

$$\cdot \left\{a\left[-A(\alpha) + R_e(1-\cos\theta)\right] + b R_e \sin\theta\cos\phi + c R_e \sin\theta \sin\phi\right\} \cdot$$

$$\cdot \cos\psi \cdot \left\{\frac{1}{\left[A(\alpha) + R_e(1-\cos\theta)\right]^2 + R_e^2 \sin^2\theta}\right\}^{3/2} R_e^2 \sin\theta \, d\phi \, d\theta , \quad (17)$$

where

S = solar constant (440 BTU/hr/ft^2)

alb = albedo factor (0.35)

ψ = angle between the solar vector S and the normal to dA_e, N_e,

Cos ψ may be obtained from:

$$\cos\psi = S \cdot N_e$$

$$= \cos(\nu-\alpha)\cos\theta\sin\lambda + \sin(\nu-\alpha)\sin\theta\cos\phi\sin\lambda + \cos\lambda\sin\theta\sin\phi . \quad (18)$$

The area of the earth that contributes to the albedo input is the surface common to the sunlit part of the earth and the part of the cap visible from the plate. The remaining area visible from the plate but receiving no sunlight contributes nothing to the heat input. This is accounted for in the numerical integration by deleting inputs when cos ψ is negative.

The average albedo flux received by the plate per rotation about the spin axis is

$$q_{A_{av.}} = \frac{1}{2\pi}\int_0^{2\pi} q_A \, d\kappa . \quad (19)$$

CALCULATION OF DIRECT SOLAR FLUX

The calculation of direct sunlight involves the determination of the instantaneous projected area of the plate with respect to the solar vector:

$$q_{SR} = S(S \cdot N)$$

$$= S\left[a\cos(\nu-\alpha)\sin\lambda + b\sin(\nu-\alpha)\sin\lambda + c\cos\lambda\right] , \quad (20)$$

where S is the solar constant.

Because of its orientation the plate may or may not be facing the sun during a rotation. Negative values of $S \cdot N$ indicate that it is not facing the sun.

The average flux per spin is

$$q_{SR_{av.}} \quad \frac{1}{2\pi} \int_0^{2\pi} q_{SR} \, d\kappa \quad . \tag{21}$$

Because the orientation of the plate is fixed in space, the heat flux is constant throughout the sun-lit portion of the orbit. To determine whether or not the satellite is within the earth's shadow at any orbital position requires two simple checks.* If both of the following expressions are satisfied, the satellite received no direct input from the sun:

$$\cos \Omega < 0 \ ,$$

$$\left[R_e + A(\alpha)\right] \cdot | \sin \qquad R_e \ ,$$

where Ω is the angle between the solar vector S and X',

$$\cos \Omega = S \cdot i' \ ,$$

$$\cos \Omega = \cos (\nu - \alpha) \sin \lambda \ .$$

APPLICATION

Hypothetical geometric configurations (Figure 5) have been chosen to illustrate the use of the equations. The external surfaces are represented by the indicated normal vectors.

*Katz, A. J., op. cit.

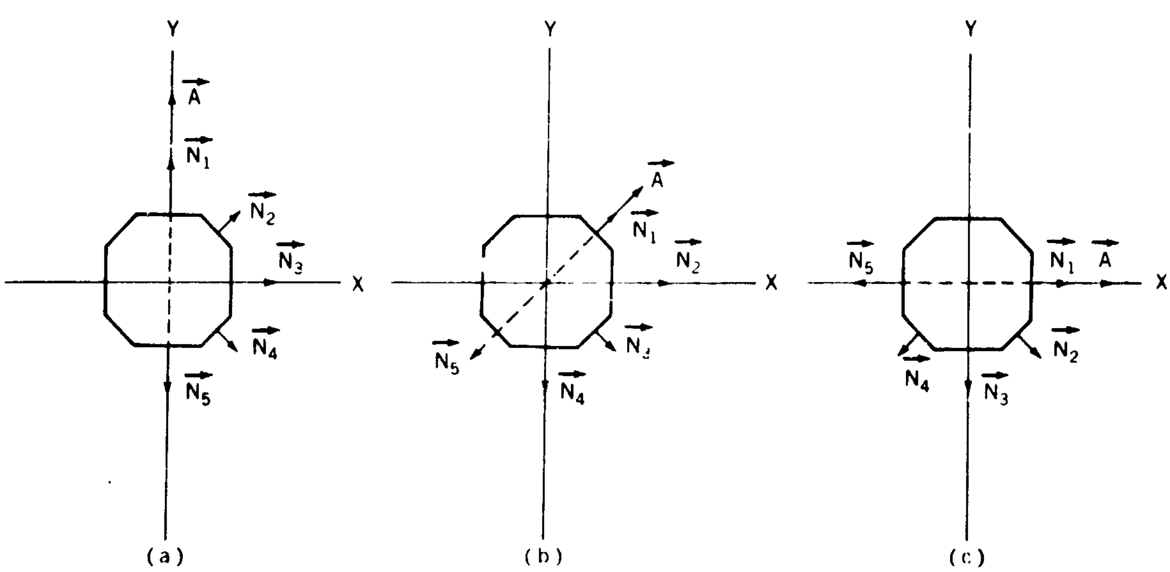

Figure 5—Geometrical configurations.

The three sketches represent three spin axis orientations.

Circular orbits of 150, 550, 1050, 2000, and 5000 statute miles, in which the solar vector lies in the plane of the orbit (minimum sunlight), were considered. Figures 6-35 indicate the orbital variation of earthshine and albedo.* These heat fluxes represent mean integrated values per rotation at the instantaneous orbital position. The direct solar flux is constant in sunlight for a specific orientation. Appropriate values are presented in Table 1.

ACKNOWLEDGMENTS

The author wishes to express gratitude to Mr. Frank Hutchinson and Mr. Henry Hartley for the IBM 7090 program and the data presentation, respectively.

Table 1
Mean Solar Heat Flux per Rotation*

δ (degrees)	β (degrees)	$Q_{SR,av.}$ (BTU/hr/ft^2)
90	90	0.0
90	45	99.0
90	0	140.0
90	315	99.0
90	270	0.0
45	45	311 0
45	0	220.0
45	315	99.0
45	270	0.0
45	225	0.0
0	0	440.0
0	315	311.0
0	270	0.0
0	225	0.0
0	180	0.0

*The data presented represent the instantaneous daylight heat flux impinging upon the rotating faces of the configuration in Figure 5 The sun in all cases is parallel to the X axis; μ, γ, and λ are 90 degrees.

*The mathematical model assumed the earth cap to be comprised of 512 elemental areas. The curves are based primarily on calculations made at 22.5 degree increments throughout the orbit Because of this, the peaks in some of the albedo curves were estimated. It should be noted that, because of the configurations chosen, the orbital heat fluxes in several cases are identical except for angular displacement.

(Manuscript received June 26, 1963)

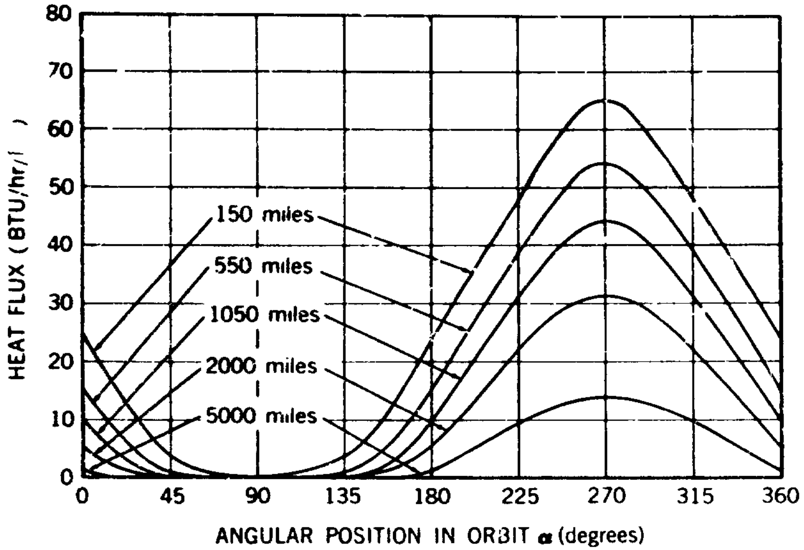

Figure 6—Earth-emitted radiation for circular orbits, δ = 90 degrees, β = 90 degrees.

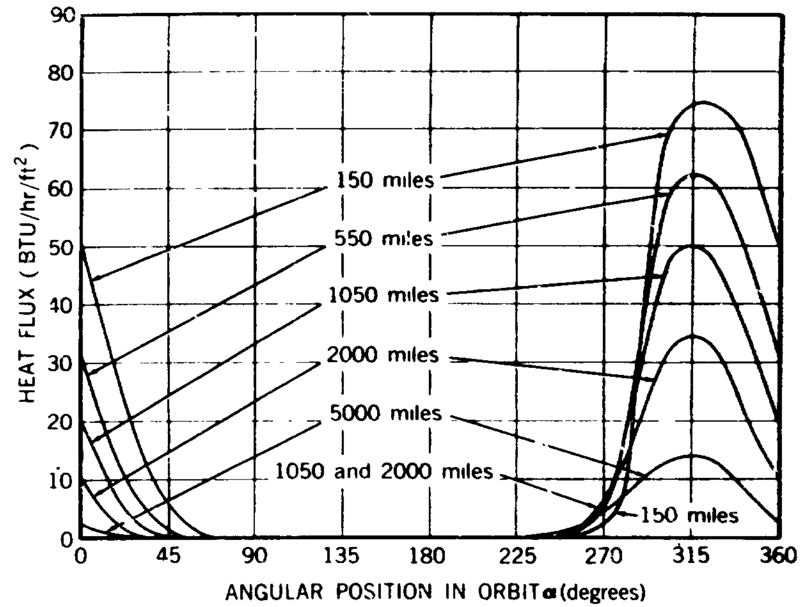

Figure 7—Albedo for minimum sunlit circular orbits, δ = 90 degrees, β = 90 degrees.

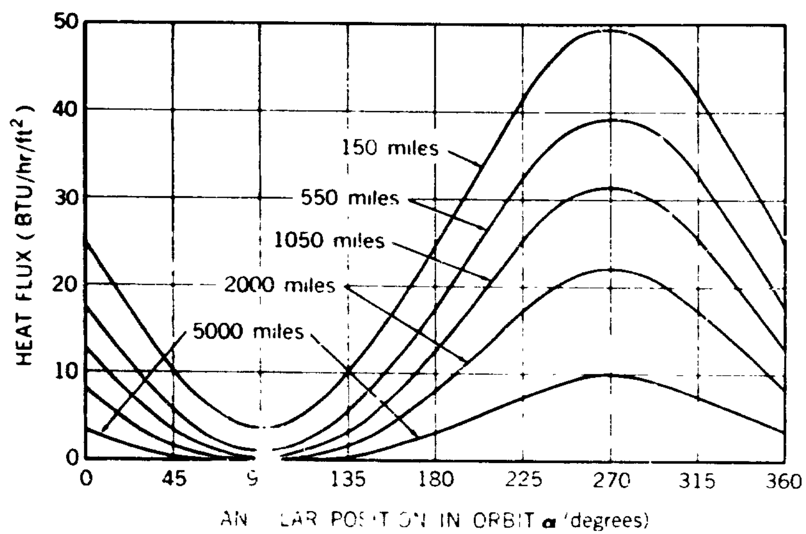

Figure 8—Earth-emitted radiation for circular orbits, δ = 90 degrees, β = 45 degrees.

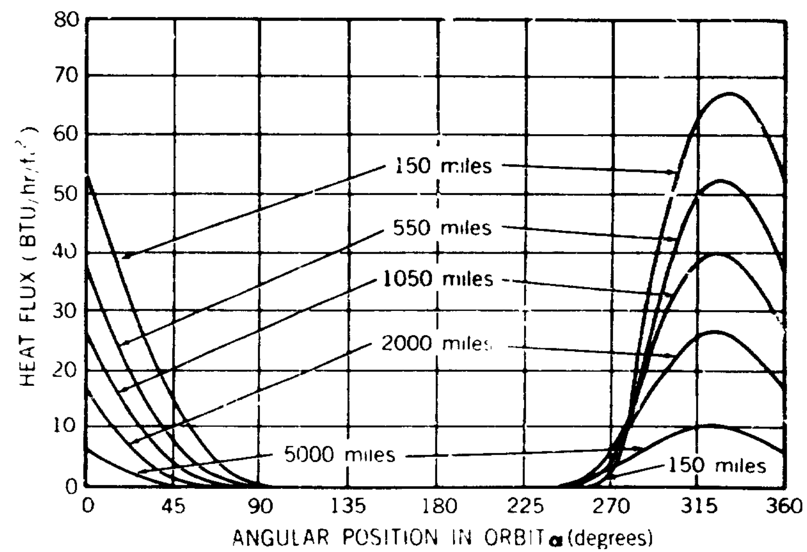

Figure 9—Albedo for minimum sunlit circular orbits, δ = 90 degrees, β = 45 degrees.

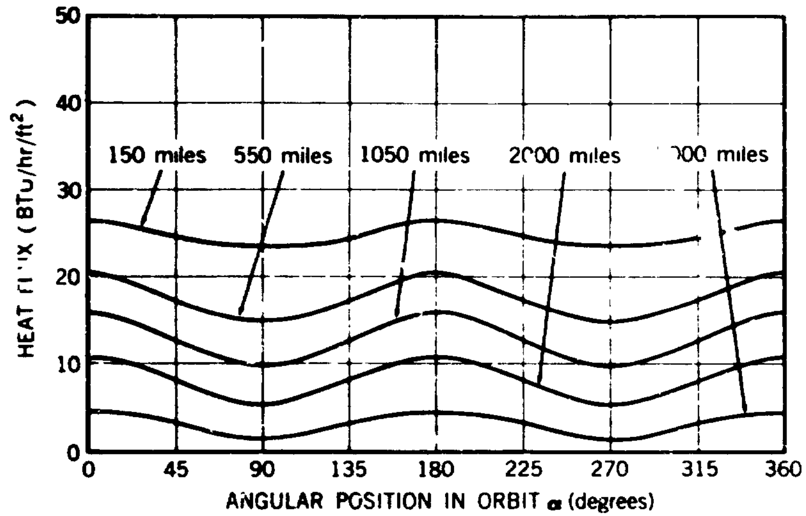

Figure 10—Earth-emitted radiation for circular orbits, δ = 90 degrees, β = 0 degrees.

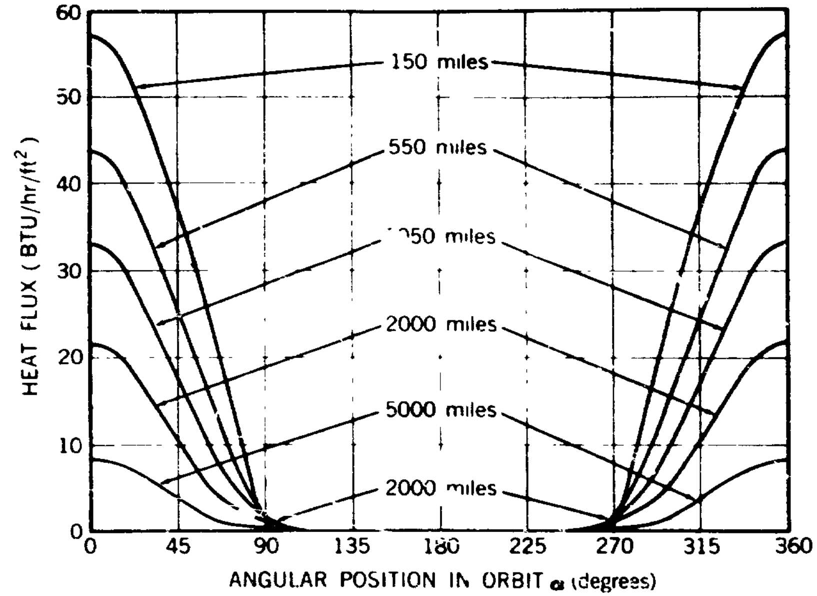

Figure 11—Albedo for minimum sunlit circular orbits, δ = 90 degrees, β = 0 degrees.

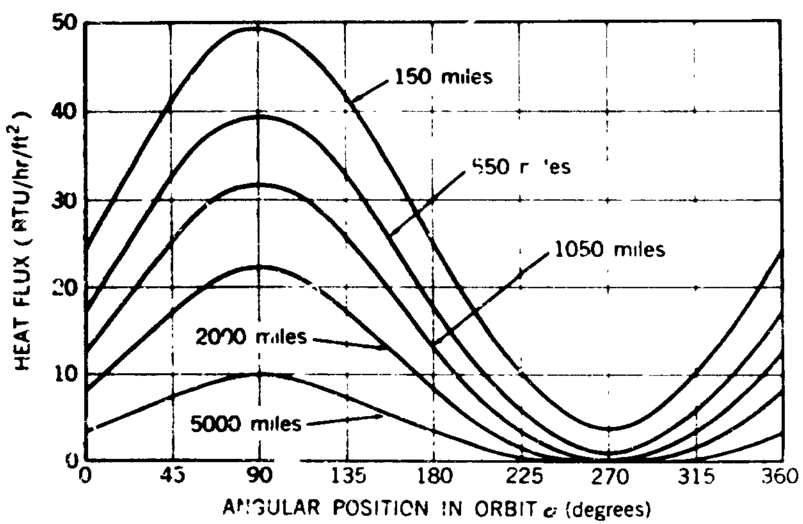

Figure 12—Earth-emitted radiation for circular orbits, δ = 90 degrees, β = 315 degrees.

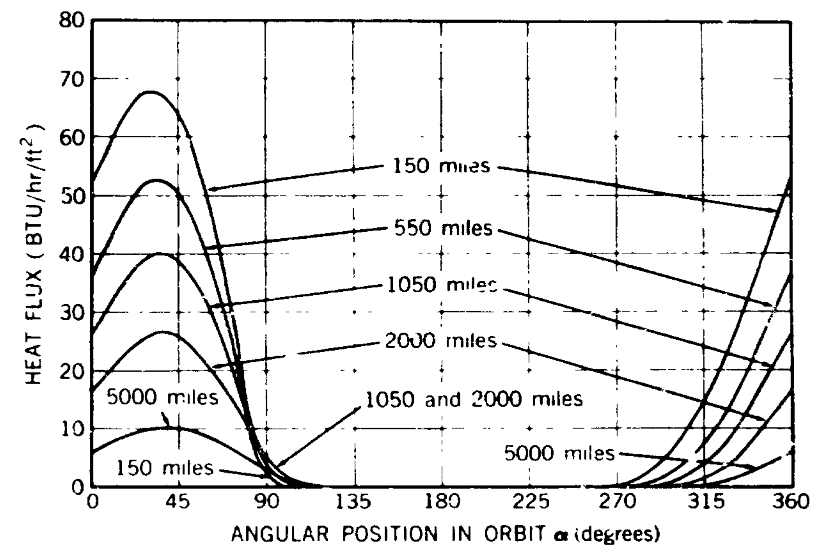

Figure 13—Albedo for minimum sunlit circular orbits, δ = 90 degrees, β = 315 degrees.

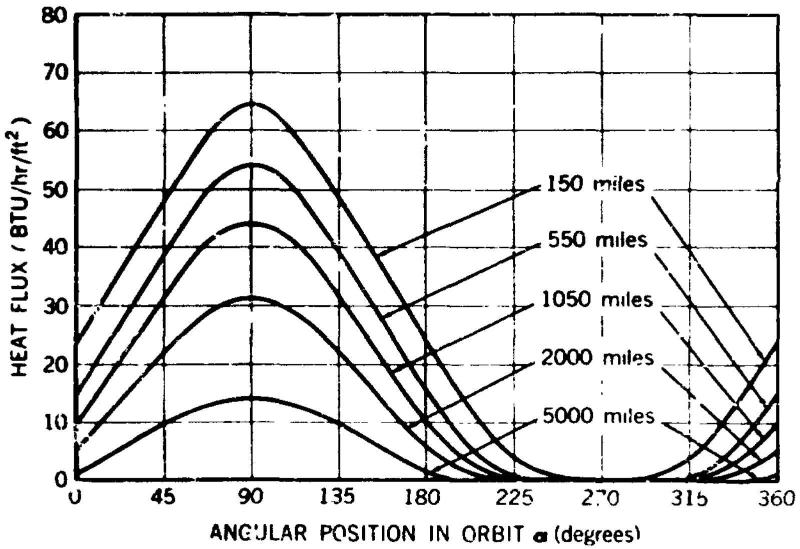

Figure 14—Earth-emitted radiation for circular orbits, δ = 90 degrees, β = 270 degrees.

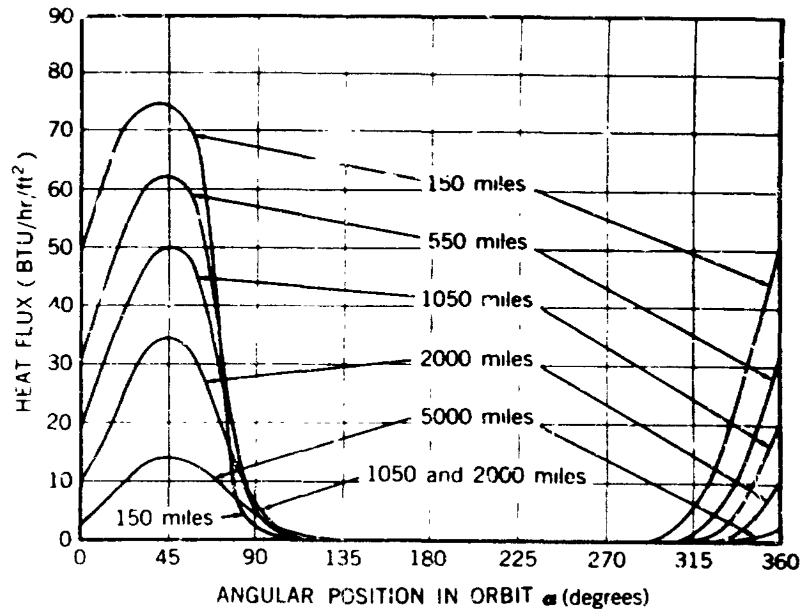

Figure 15—Albedo for minimum sunlit circular orbits, δ = 90 degrees, β = 270 degrees.

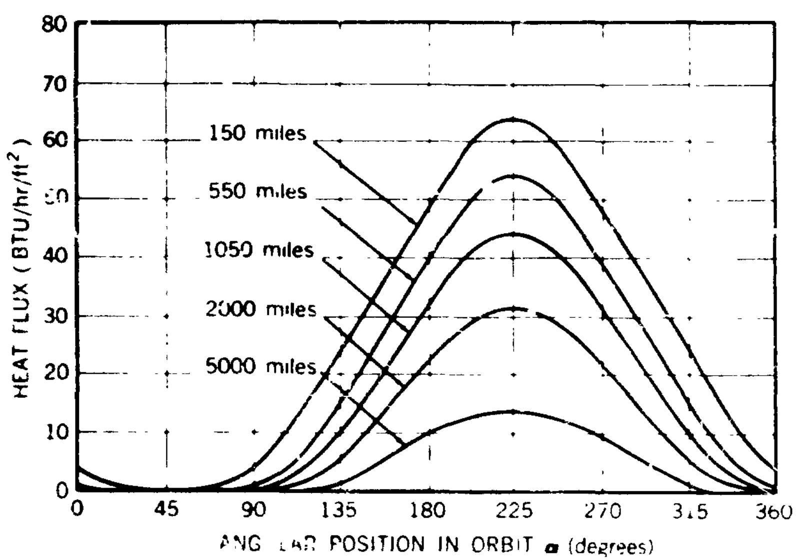

Figure 16—Earth-emitted radiation for circular orbits, δ = 45 degrees, β = 45 degrees.

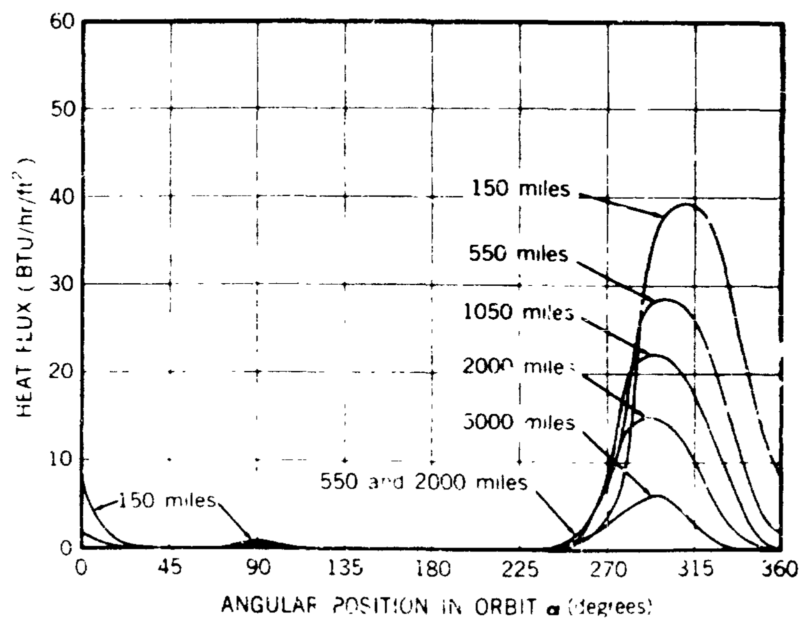

Figure 17—Albedo for minimum sunlit circular orbit, δ = 45 degrees, β = 45 degrees.

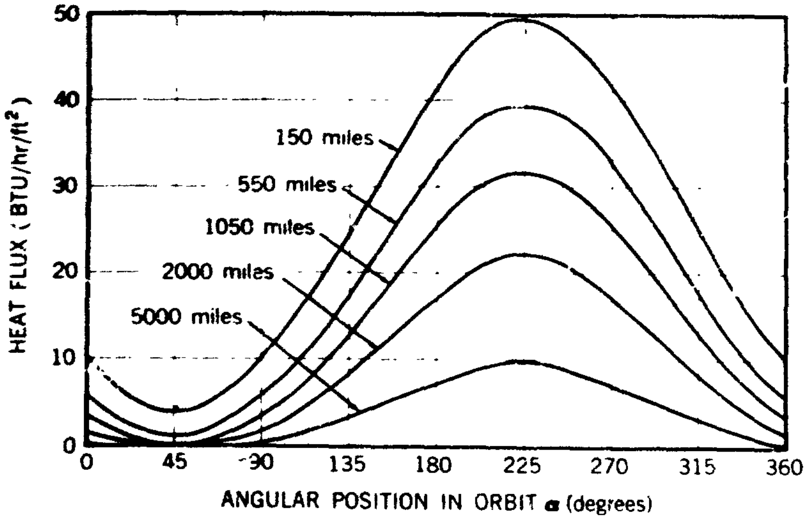

Figure 18—Earth-emitted radiation for circular orbits, δ = 45 degrees, β = 0 degrees.

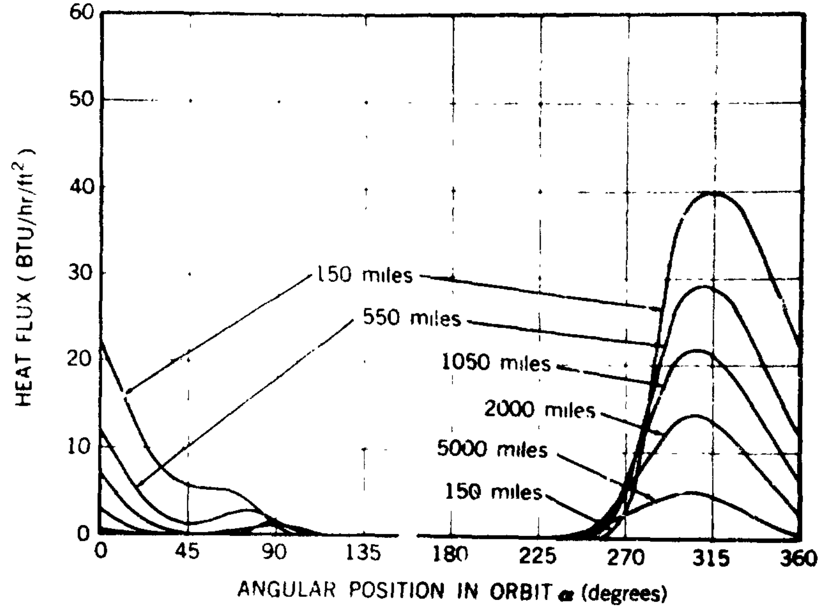

Figure 19—Albedo for minimum sunlit circular orbits, δ = 45 degrees, β = 0 degrees.

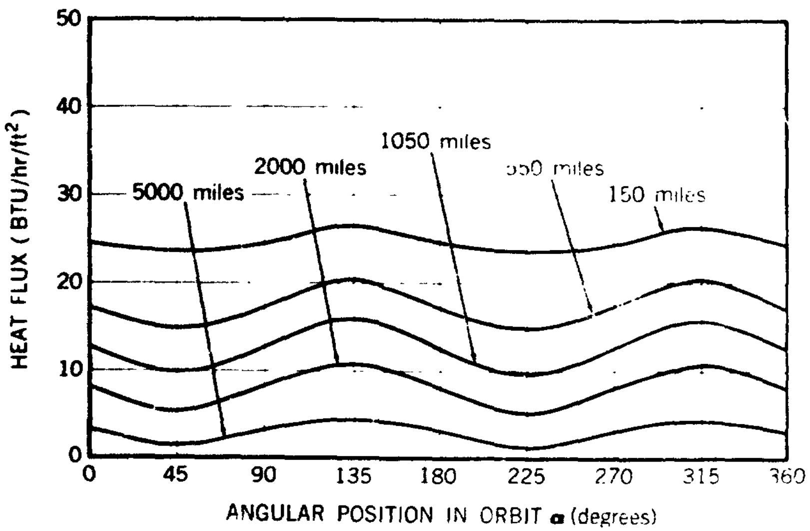

Figure 20—Earth-emitted radiation for circular orbits, δ = 45 degrees, β = 315 degrees.

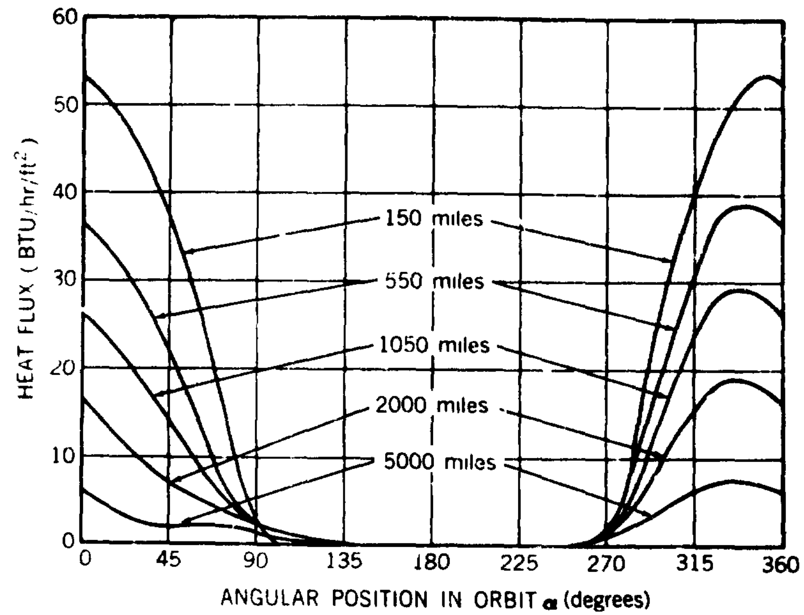

Figure 21—Albedo for minimum sunlit circular orbits, δ = 45 degrees, β = 315 degrees.

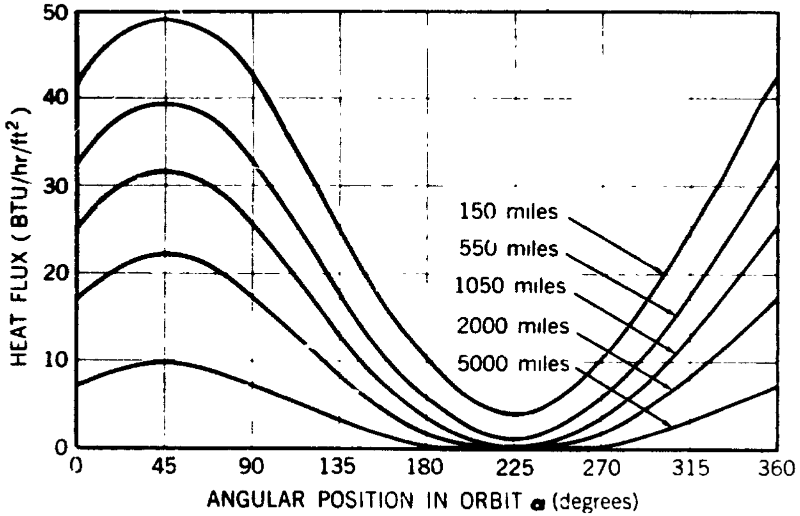

Figure 22—Earth-emitted radiation for circular orbits, δ = 45 degrees, β = 270 degrees.

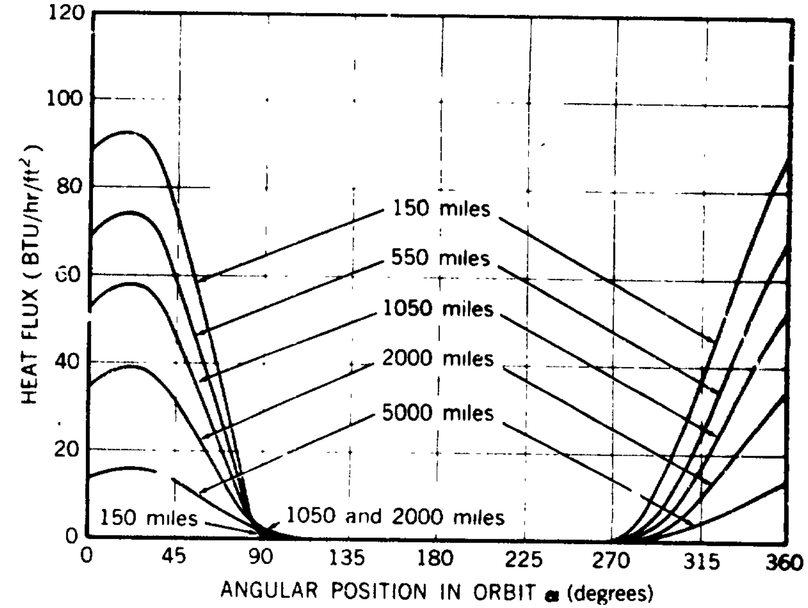

Figure 23—Albedo for minimum sunlit circular orbits, δ = 45 degrees, β = 270 degrees.

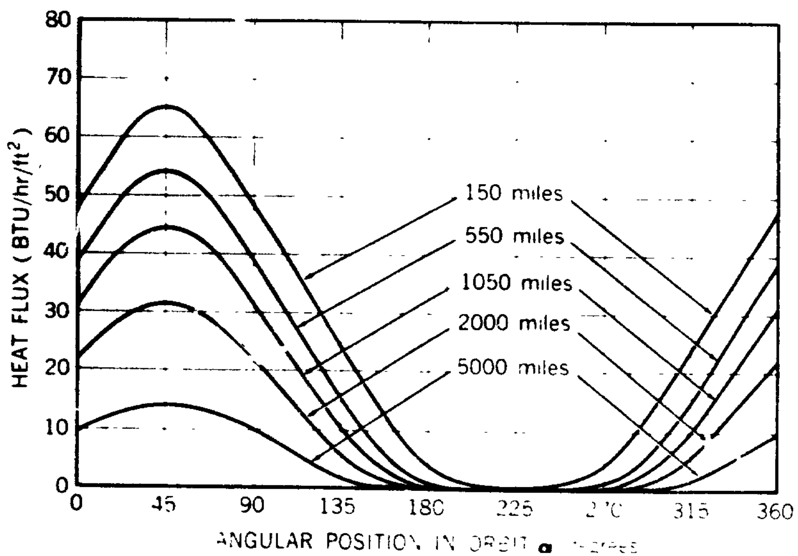

Figure 24—Earth-emitted radiation for circular orbits, δ = 45 degrees, β = 225 degrees.

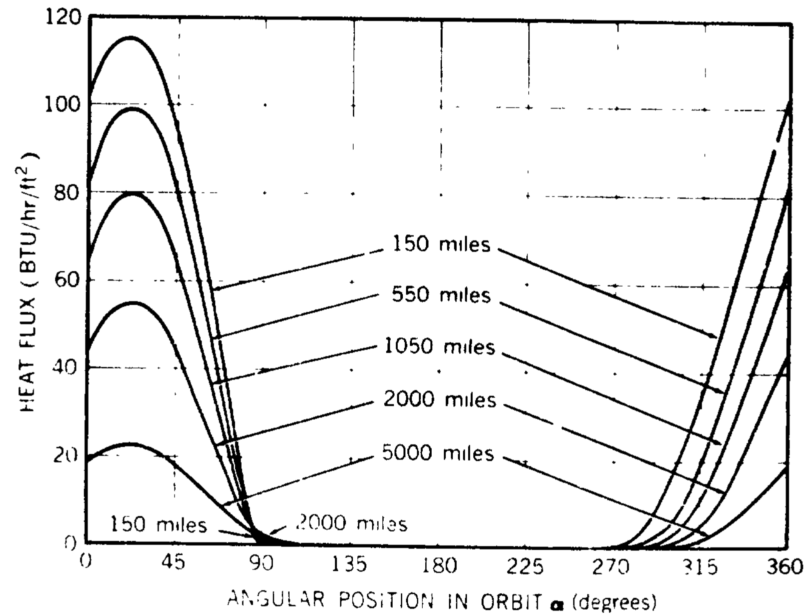

Figure 25—Albedo for minimum sunlit circular orbits, δ = 45 degrees, β = 225 degrees.

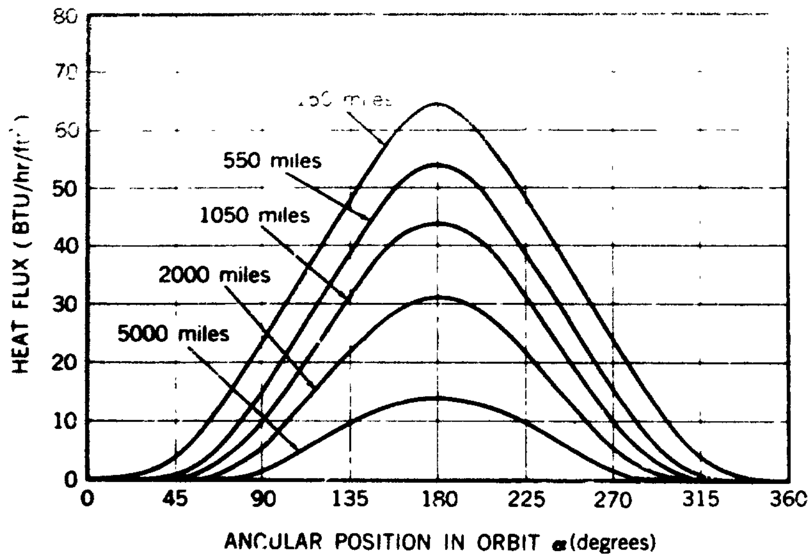

Figure 26—Earth-emitted radiation for circular orbits, $\delta = 0$ degrees, $\beta = 0$ degrees.

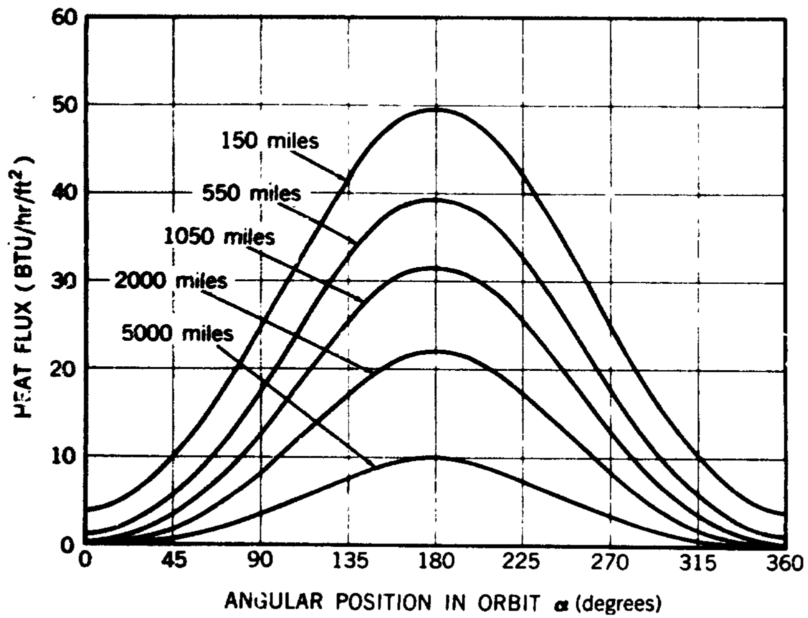

Figure 28—Earth-emitted radiation for circular orbits, $\delta = 0$ degrees, $\beta = 315$ degrees.

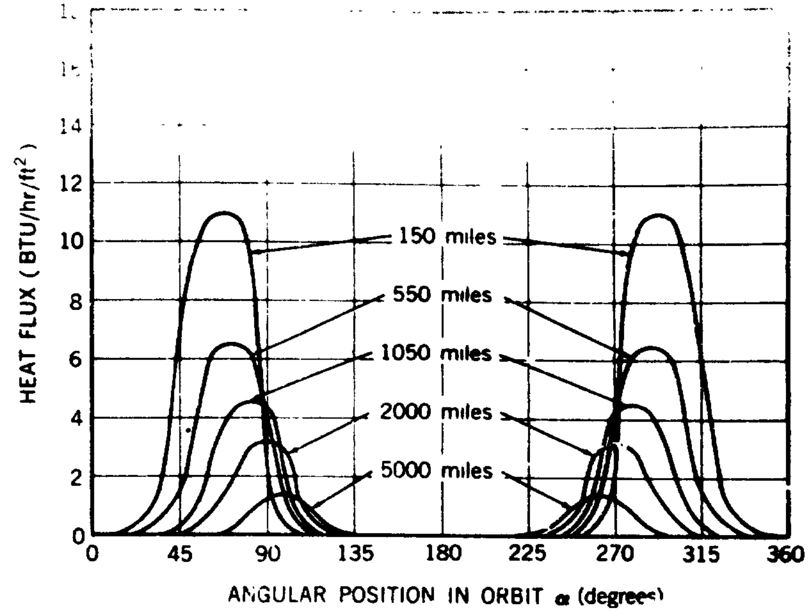

Figure 27—Albedo for minimum sunlit circular orbits, $\delta = 0$ degrees, $\beta = 0$ degrees.

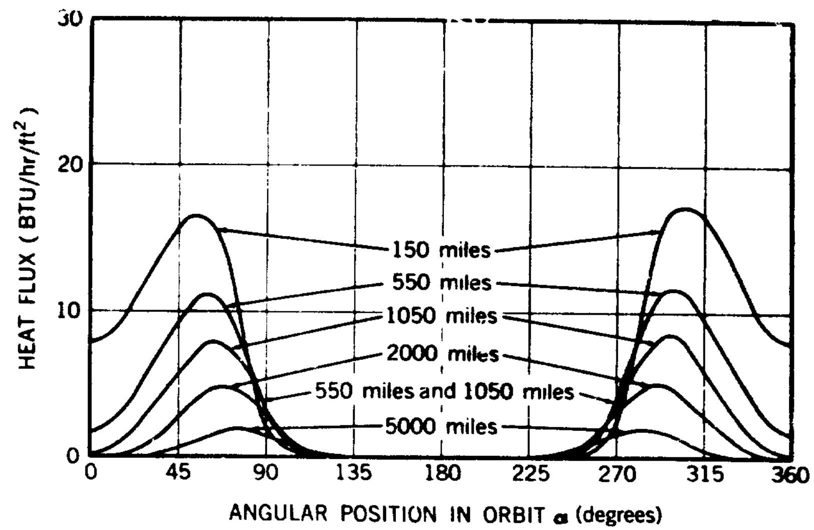

Figure 29—Albedo for minimum sunlit circular orbits, $\delta = 0$ degrees, $\beta = 315$ degrees.

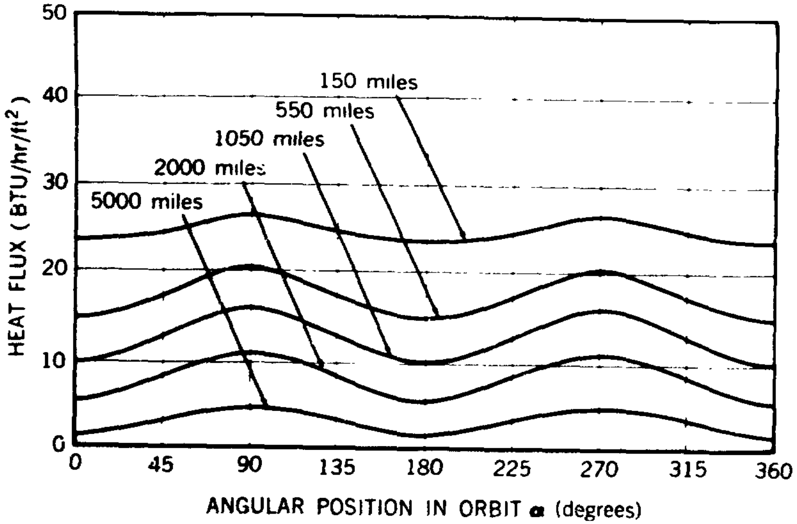

Figure 30—Earth-emitted radiation for circular orbits, δ = 0 degrees, β = 270 degrees.

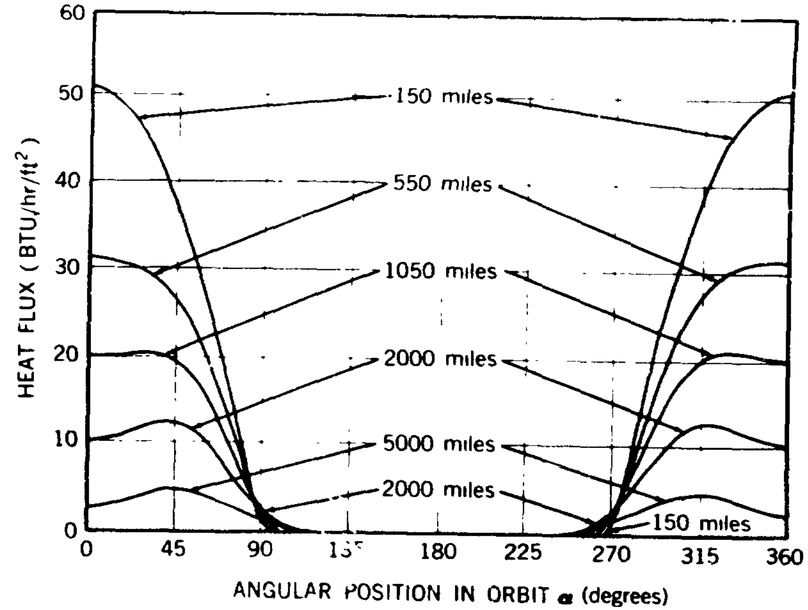

Figure 31—Albedo for minimum sunlit circular orbits, δ = 0 degrees, β = 270 degrees.

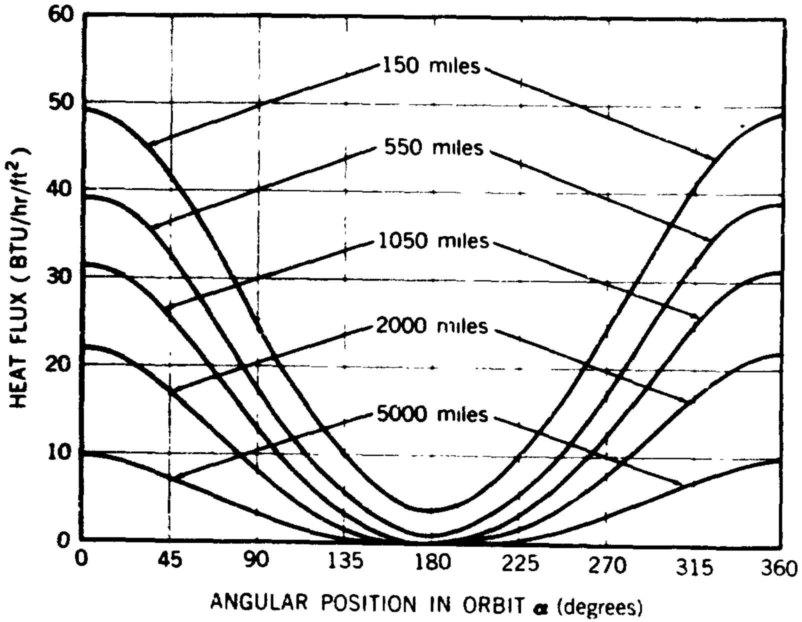

Figure 32—Earth-emitted radiation for circular orbits, δ = 0 degrees, β = 225 degrees.

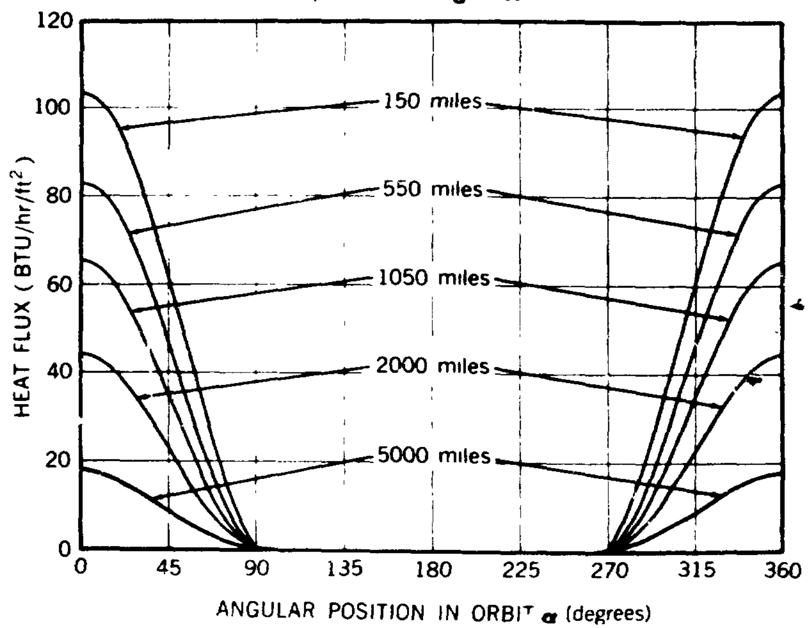

Figure 33—Albedo for minimum sunlit circular orbits, δ = 0 degrees, β = 225 degrees.

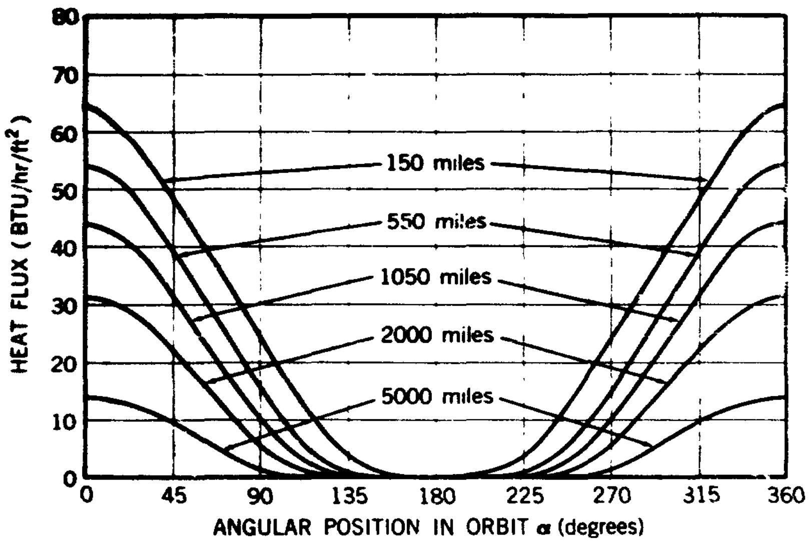

Figure 34—Earth-emitted radiation for circular orbits, δ = 0 degrees, β = 180 degrees.

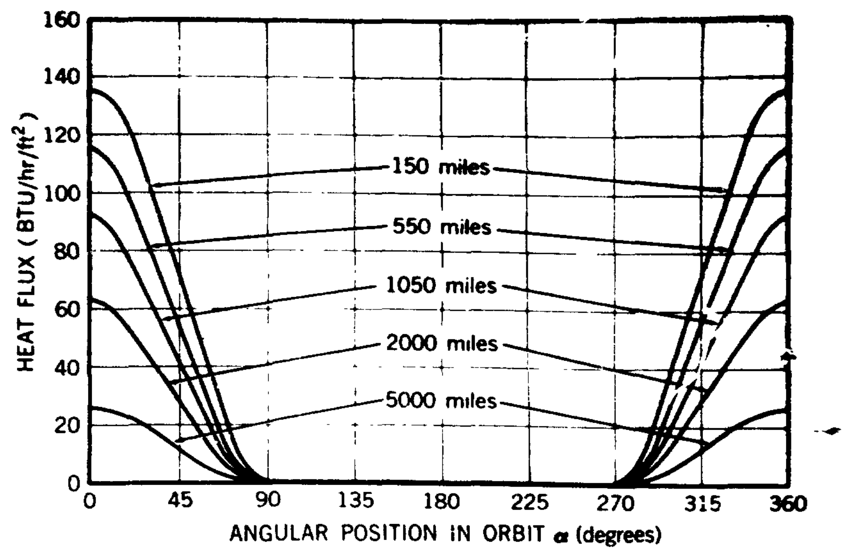

Figure 35—Albedo for minimum sunlit circular orbits, δ = 0 degrees, β = 180 degrees.